

IMPERIAL COLLEGE LONDON

A Comparison of two Cosmological Models: Inflationary Cosmology and the Cyclic Universe

Author:
Charlotte Strege

Supervisor:
Dr. Carlo Contaldi

Abstract

To explain current observations the early universe must have been incredibly flat and homogeneous. Tiny density fluctuations must have been present to seed large scale structure. Any viable model of the universe has to explain these cosmological puzzles and be able to generate a nearly flat spectrum of density perturbations, as required by microwave background data. Inflation is a period of accelerated expansion in the very early universe. Combined with the big bang model it forms the consensus model of cosmology. The cyclic model, inspired by M-theory, describes a universe undergoing an infinite sequence of cycles that start with a big bang and end in a big crunch. Each cycle includes a slowly contracting "ekpyrotic" phase. Both inflation and an ekpyrotic phase can resolve the cosmological problems and lead to the required perturbation spectrum. In this paper inflationary cosmology and the cyclic model are compared. Their dynamics are described using scalar fields and their solutions to the cosmological problems are presented. Strengths and weaknesses of the models are compared; open issues and conceptual problems are identified. The observational signatures are contrasted and confronted with experiments. Future possibilities to distinguish between the models due to differing predictions for non-gaussianity and gravitational waves are discussed.

Submitted in partial fulfilment of the requirements for the degree of Master of Science of Imperial College London

September 24, 2010

Contents

1	Introduction	2
2	The Cosmological Problems	8
3	Inflation	12
3.1	The Inflationary Universe	12
3.2	Inflation and the Cosmological Problems	15
3.3	Generation of Cosmological Perturbations	19
4	The Ekpyrotic/Cyclic Universe	33
4.1	The Ekpyrotic Phase	35
4.2	The Cyclic Universe	37
4.3	The Ekpyrotic/Cyclic Universe and the Cosmological Problems	44
4.4	Generation of Cosmological Perturbations	47
5	Inflationary Cosmology versus the Cyclic Universe	63
5.1	Strengths and Problems of the Models	64
5.2	Experimentally Testable Predictions	72
6	Conclusions	79

1 Introduction

The standard model describing the evolution of the universe is the big bang model. In this model the universe originated in an infinitely hot and dense state and has been expanding and cooling ever since. The big bang theory is extremely successful and can accurately describe the evolution of the universe from the time of nucleosynthesis until today. However, the behaviour of the early universe preceding nucleosynthesis is uncertain. In the standard big bang model the universe was radiation-dominated from the beginning until at some point matter domination took over. During these two stages the expansion of the universe was decelerating. While this is a very good description of the long-term evolution of the universe, it has recently been discovered that the expansion of the universe is accelerating [1, 2]. The acceleration is assumed to be due to some mysterious form of self-repulsive energy, called dark energy. This discovery was not predicted and has so far been difficult to accommodate by the big bang model.

By combining the standard big bang model with observations of our universe one can extrapolate back in time to find the approximate properties of the very early universe. To lead to a universe like ours the early universe must have been extremely homogeneous, isotropic and flat. Additionally, as discovered by the WMAP [3] and COBE satellites [4, 5], tiny density fluctuations with a nearly gaussian, close to scale-invariant spectrum must have been present. The origin of these fluctuations is unknown. Therefore, to be in accordance with observations the early universe must have been in a very special state, which requires extreme fine-tuning of initial conditions. Explaining these features is one of the main issues of big bang cosmology. Any successful cosmological model must offer a convincing argument as to why the early universe was so flat and homogeneous, as well as providing a mechanism to generate the required spectrum of density perturbations.

The most widely accepted mechanism to solve these cosmological problems is a brief period of rapid accelerated expansion in the very early universe, occurring shortly after the big bang and preceding nucleosynthesis. This so-called period of inflation can explain the properties of the observed universe. It is the most popular theory describing the early universe and can easily be incorporated into the big bang theory, leading to the current consensus model of cosmology.

Inflation first became popular when its potential to solve the major cosmological problems was realised by Guth in 1981 [6]. The original model describes

exponential expansion occurring in a false vacuum, a state that is completely empty but that has a non-zero energy density. It includes a first-order phase transition from a supercooled inflating false vacuum state to the true vacuum in which the energy density is zero. Therefore, the exponential expansion is stopped via quantum barrier penetration which results in bubbles of true vacuum appearing. These bubbles can collide, leading to a hot universe. Unfortunately, it was soon found that such a scenario does not include a successful graceful exit into the Friedmann stage and would eventually lead to a highly inhomogeneous universe [7, 8]. In 1982 a different version of inflation, called new inflation, was proposed by Linde [9, 10, 11], and Albrecht and Steinhardt [12]. The main concept of this version is that exponential expansion of the universe occurs while a scalar field is slowly rolling down its potential towards the global minimum, away from an unstable initial state. Therefore, in contrast to old inflation, the important part of inflation occurs away from the unstable false vacuum. New inflation, however, also turned out to not be a desirable scenario, since it suffers from a number of fine-tuning problems. In 1983 it was replaced by chaotic inflation [13]. Chaotic inflation also relies on the slow-roll of a scalar field down a potential. However, while both new and old inflation require that the universe is in a state of thermal equilibrium before inflation begins, chaotic inflation includes no such assumption. In fact, for chaotic inflation the initial conditions can be almost completely arbitrary [13]. As long as a sufficiently flat potential is present chaotic inflation can occur. It thus avoids the problems faced by the other two scenarios and is now the most widely accepted model of inflation.

The inflationary scenario discussed in this paper is chaotic inflation. The dynamics of this scenario can be modelled using a scalar field which is slowly rolling down a positive, flat potential in a Friedmann-Robertson-Walker universe. Since the universe grows exponentially during inflation, the observable universe originated from a very small region. Using this exponential expansion of space inflation can explain the flatness and large-scale homogeneity of the universe, as well as the absence of topological defects. Most importantly, during inflation quantum fluctuations of the scalar field are amplified and stretched beyond the horizon, where they are frozen. The perturbations re-enter the horizon during the standard big bang phase and seed the formation of structure. Inflation can thus explain the origin of large-scale structure as well as the observed anisotropy of the cosmic microwave background (CMB). The density perturbation spectrum predicted by inflation is almost scale-invariant with a nearly gaussian distribution [14, 15, 16, 17, 18], which is in accordance with recent observations [3, 19]. Inflation also predicts a nearly scale-invariant spectrum of gravitational waves which has not yet

been observed.

Even though inflation is an incredibly successful theory that is in excellent agreement with observations, it contains some unresolved conceptual problems and has not conclusively been tested, yet. This leads to the question if inflation's successes in solving the cosmological problems are truly unique. The achievements of the consensus model should not blind us to the fact that there might be an alternative cosmological model that can more accurately account for the current state of the universe, while also solving the problems of standard big bang cosmology. In this review we present a set of models inspired by string and M-theory that might achieve this, the ekpyrotic and cyclic models of the universe. While many other alternative models exist, this scenario is commonly seen as the most convincing alternative to the consensus model. To quote Andrei Linde, one of the main developers of chaotic inflation: "The ekpyrotic/cyclic scenario is the best alternative to inflation that I am aware of" [20]. This is why we choose this model to contrast with inflationary and big bang cosmology.

The ekpyrotic universe can solve the problems of standard big bang cosmology and generate a nearly scale-invariant spectrum of perturbations that agrees with observations without requiring an era of accelerated expansion in the early universe. Instead, it relies on a period of ultra-slow contraction, the ekpyrotic phase, occurring before the big bang. During this phase the Hubble horizon is rapidly decreasing, while quantum fluctuations remain nearly constant in scale. Therefore, quantum fluctuations can leave the horizon and re-enter it after the big bang, leading to the formation of structure in the post-big bang universe. A period of "ekpyrosis" is involved in a number of different cosmological models. The first attempt to use a pre-big bang ekpyrotic phase to explain the state of the universe today was made when the ekpyrotic model of the universe was proposed by Khoury, Ovrut, Steinhardt and Turok in 2001 [21]. This model is embedded in heterotic M-theory [22, 23, 24, 25, 26] and relies on a five-dimensional braneworld scenario in which two boundary branes approach each other along the fifth dimension due to an attractive potential. The big bang corresponds to a collision of the two branes, one of which represents our universe. The model can be described in the four-dimensional effective theory using a scalar field rolling down a steep, negative potential. It was soon realised that via this model a scale-invariant spectrum of curvature perturbations could not be produced [27]. Instead, an entropic mechanism relying on the presence of two scalar fields was introduced to generate the required spectrum [28].

An important extension of the ekpyrotic scenario is the cyclic model of the universe which was introduced by Steinhardt and Turok in 2002 [29, 30]. In this model the universe is going through an infinite sequence of contraction and expansion. Consecutive cycles are connected by a big crunch/big bang transition, corresponding to a collision of two boundary branes, as in the ekpyrotic model. After each collision the branes separate, but eventually start attracting each other again. Each cycle includes an ekpyrotic phase, a hot big bang phase and a period of quintessence domination. Therefore, the model incorporates the recently observed accelerated expansion. The cyclic model that employs the entropic mechanism of density perturbation generation is known as the phoenix universe [31]. In this scenario after each bounce only a very small fragment of the universe re-emerges as a flat, expanding phase. Its reproduction crucially depends on the presence of an extended period of dark energy domination [31, 32]. Just like the ekpyrotic model, the cyclic model can be described in four dimensions using a scalar field evolving along its potential. The cyclic potential takes both positive and negative values.

The main problem facing ekpyrotic and cyclic models is matching the conditions achieved during ekpyrosis across the big crunch/big bang singularity. At this singularity the higher dimensional framework becomes important and a better understanding of string theoretical effects is required to accurately describe the transition from contraction to expansion. Due to the lack of a consistent theory of quantum gravity, models involving a non-singular bounce became popular. The most important such scenario is the new ekpyrotic universe which was introduced in 2007 [33]. This scenario reverses from contraction to expansion before the quantum gravity regime is reached. It requires a violation of the null energy condition which is achieved by including a ghost condensate phase. Unfortunately, some serious problems with the new ekpyrotic model have recently been discovered [34, 35]. Therefore, this paper will focus on the cyclic universe scenario, in which the bounce is singular and string theoretical effects are important [36]. For the model to have predictive power we will assume that the bounce preserves the properties of the universe generated during ekpyrosis. Using the entropic mechanism the cyclic model can then generate the nearly scale-invariant spectrum of density perturbations that is observed today. In contrast to inflation, the non-gaussian contribution to this spectrum is quite large [37] and the predicted gravitational wave spectrum is strongly blue [38].

While the consensus model and the cyclic model are conceptually very different, both models agree with current observational data [3]. It will be future

observations that decide which of the two models is correct. We are living in a very exciting time for cosmology. For the first time in history observations can be used to probe the physics of the very early universe. Ever since COBE discovered anisotropies in the cosmic microwave background in 1992 [4] models of the universe have been tested using precise measurements of the cosmological perturbation spectra. Satellite experiments like WMAP and the future Planck mission can probe the microwave background to unprecedented accuracy. Cosmology no longer is a purely theoretical field, but in the last two decades became a precision science that uses experimental data to test the existing theories. Within the next few years it will be possible to detect signatures of non-gaussianity and maybe even gravitational waves to a high enough accuracy to determine which one of the two cosmological models presented in this paper, if any, is correct.

Given these exciting prospects, this is an excellent time to contrast the cyclic and inflationary cosmologies, uncover their theoretical weak points and compare their observationally testable predictions. The purpose of this paper is to provide such a comparison. It is emphasised that we are not aiming to give a detailed review of the two models. For such a review of inflation one should see e.g. [39, 40]. An excellent review of the ekpyrotic/cyclic scenarios is given in [41]. The main aim of this paper is to compare, not to review. To experts in cosmology it will be obvious that not all aspects of the models are presented in full detail and that the focus is on parts that are needed for an accurate comparison. For example, this paper concentrates on the simple, single-field model of inflation and almost completely ignores multi-field inflationary scenarios. Also, as stated earlier, we will focus on the cyclic model of the universe and only rarely refer to the original ekpyrotic model. Additionally, after a brief discussion of the higher-dimensional embedding the model will mostly be presented in terms of the four-dimensional effective theory, relying on a scalar field evolving along its potential. This is appropriate for a comparison of the cyclic model with the consensus model, since inflation is described using the same ingredients.

This paper is organised as follows. In section 2 the cosmological problems of the standard big bang model are presented. In section 3 the concept of single-field inflation is introduced. It is explained how inflation solves the cosmological problems, the spectra of scalar and tensor perturbations are calculated and the non-gaussian corrections are discussed. The cyclic model of the universe is described in section 4. The dynamics of the ekpyrotic phase and its solutions to the problems of big bang cosmology are presented. The discussion is extended to two fields and the generation of curvature pertur-

bations is analysed. Predictions for the degree of non-gaussianity and the spectrum of gravitational waves are given. Section 5 focuses on the comparison of the two models. Their strengths and weaknesses are explained and the most urgent open issues are identified. Their observationally testable predictions for scalar and tensor perturbations as well as non-gaussian corrections are contrasted. The main conclusions are presented in section 6.

2 The Cosmological Problems

Flatness problem

The present-day universe is very close to being flat. In a decelerating universe this requires the universe to be even closer to flat at earlier times. This turns out to be a very restrictive requirement as can be seen from a simple calculation. The first Friedmann equation reads ¹

$$H^2 + \frac{k}{a^2} = \frac{8\pi G}{3}\rho, \quad (1)$$

where $a(t)$ is the scale factor, $H(t) = \dot{a}(t)/a(t)$ is the Hubble parameter, with dotted quantities implying a time derivative $\dot{a}(t) = da(t)/dt$, $\rho(t)$ is the energy density and k is a constant, with $k = -1, 0, 1$ for an open, flat and closed universe respectively. G is Newton's constant. This can be rewritten using the cosmological parameter $\Omega(t) = \rho(t)/\rho^{cr}(t)$, with ρ^{cr} the critical energy density that would make the universe spatially flat

$$\rho^{cr} = \frac{3H^2}{8\pi G}. \quad (2)$$

The first Friedmann equation then becomes

$$\Omega(t) - 1 = \frac{k}{(aH)^2}. \quad (3)$$

This implies that the cosmological parameter at some earlier time t_i can be calculated as

$$\Omega(t_i) - 1 = (\Omega(t_0) - 1) \frac{H^2(t_0)a^2(t_0)}{H^2(t_i)a^2(t_i)}, \quad (4)$$

where t_0 is the age of the universe today. It is known that today $\Omega(t_0) = 1.02 \pm 0.02$ [42] ². In a matter dominated universe the scale factor grows as $a \propto t^{2/3}$. Assuming that the age of the universe today is $t_0 \approx 4.3 \cdot 10^{17}s$ and at recombination $t_r \approx 1.2 \cdot 10^{13}s$, then $\Omega(t_r) - 1 < 10^{-4}$. The cosmological parameter at recombination was very close to unity and thus the universe was very close to being flat. This trend continues as one considers earlier times. In a radiation dominated universe the scale factor grows as $a \propto t^{1/2}$. Assuming the universe was radiation dominated from the Planck time $t_{pl} \approx 10^{-43}s$

¹In the following natural units $\hbar = c = 1$ are used

²In fact, recent data give the more precise value of $\Omega(t_0) = 1.0023^{+0.0056}_{-0.0054}$ [3]. However, to estimate the extent of the flatness problem the precision of the value given is sufficient.

until matter-radiation equality occurring at $t_{eq} \approx 2.0 \cdot 10^{12}s$, then at the Planck time $\Omega(t_{pl}) - 1 < 10^{-60}$. This corresponds to initial conditions that are extremely fine-tuned. While this result is by no means unphysical, initial conditions leading to such an extremely flat universe seem to demand an explanation.

To emphasize the extent of the problem one should note that

$$\Omega(t_{pl}) - 1 = \frac{\rho(t_{pl}) - \rho_{cr}(t_{pl})}{\rho_{cr}(t_{pl})} < 10^{-60}. \quad (5)$$

Thus, if the initial energy density was higher or lower than ρ_{cr} by only $10^{-59}\rho_{cr}$, the universe would either have recollapsed a long time ago or become empty so early that life as we know it would not exist.

Homogeneity/Horizon problem

The universe we observe today is very homogeneous and isotropic. Since it consists of many patches that were out of causal contact at earlier times it is unclear why such a high degree of homogeneity is observed on the horizon scale.

The comoving particle horizon is the maximum distance a photon could have travelled since the beginning of the universe until today. Any point that is outside this horizon today has never been in causal contact with the observable universe. The particle horizon d_p is defined as

$$d_p(t) = c \cdot a(t) \int_0^t \frac{dt}{a(t)}, \quad (6)$$

where it was assumed that the initial singularity occurs at $t = 0$ and the speed of light c was restored. This factor will be written explicitly throughout this section, since it has to be included in the calculations in order to obtain correct results. After inserting $a \propto t^n$ into (6) it reads

$$d_p(t) = \frac{ct}{1-n}. \quad (7)$$

One should note that this is proportional to the Hubble radius $1/H(t) \propto t$. A radiation dominated universe is described by $n = 1/2$ which leads to $d_p(t) = 2 \cdot ct$. To get a rough idea of the extent of the horizon problem we can assume that the universe was radiation dominated throughout its entire

lifetime. Using the times given in the discussion of the flatness problem the particle horizon at these times can be found. The particle horizon today is then given by $d_p(t_0) \approx 8.3$ Gpc. The particle horizon at recombination is roughly $d_p(t_r) \approx 230$ kpc. Therefore, the universe we see today was made up of many causally disconnected regions at recombination. However, the CMB is known to be very homogeneous and isotropic with temperature fluctuations of at most $\mathcal{O}(10^{-4})T$. Furthermore, the phase of the acoustic oscillations is the same in all of the previously causally disconnected patches. There is no causal physical process that could be responsible for this homogeneity.

The situation is aggravated when looking at the universe at the Planck time. To obtain a rough estimate of the extent of the horizon problem one compares the size of our observable universe at the Planck time with the size of a causal region at that time, again assuming the universe is radiation dominated, so that $d_p(t) = 2 \cdot ct$. The size of our homogeneous domain at some earlier time t_i is proportional to the scale factor at that time:

$$d_h(t_i) \approx 2 \cdot ct_0 \frac{a(t_i)}{a_0}, \quad (8)$$

where $2 \cdot ct_0 \approx 8.3$ Gpc is the present horizon scale and $d_h(t_i)$ is the size of our homogeneous domain of the universe at time t_i . One can compare this to the particle horizon at time t_i , given by $d_p(t_i) \approx 2 \cdot ct_i$. Taking $a(t) \propto t^{1/2}$ one finds that at the Planck time

$$\frac{d_h(t_{pl})}{d_p(t_{pl})} \approx \left(\frac{t_0}{t_{pl}} \right)^{1/2} \approx 10^{30}. \quad (9)$$

This means that the homogeneous, isotropic domain of the universe observed today was made up of approximately $(10^{30})^3 = 10^{90}$ causally disconnected regions at the Planck time. To produce such a homogeneous and isotropic domain the matter distribution had to be extremely homogeneous in each of these regions. While the discussion above has focussed on a radiation dominated universe it is clear that a problem of such extent will still exist in a universe where at some stage matter domination took over. No causal physical process could have smoothed out inhomogeneities to create such homogeneous patches.

Origin of large-scale structure

If a solution to the homogeneity problem is found it still needs to be explained how galaxies, galaxy clusters and other large scale structures observed today

could form from such a homogeneous universe. More specifically, the origin of the primordial inhomogeneities that seed the density fluctuations that are observed both in the large scale structure of the universe and in the CMB has to be found. A theory explaining structure formation should also explain the almost perfect scale invariance in the amplitudes of the CMB anisotropies found by WMAP [3].

The problem of the origin of large-scale structure can be reformulated using the Hubble radius $1/H$. In a decelerating universe, such as the universe in the big bang theory, this radius is always increasing. The Hubble radius is an important scale, since only inside this radius causal physics can operate. As it increases during the standard big bang scenario, more and more scales become smaller than the Hubble radius and enter the horizon. Once they crossed the horizon they stay inside it for all time. This leads to the question of how these perturbations that continuously enter the horizon were created.

Monopole problem

Most Grand Unified Theories (GUTs) and other unification models predict the existence of magnetic monopoles or other exotic heavy particles (gravitinos, Kaluza-Klein particles, etc.). Such superheavy particles could only have been produced at very high temperatures, therefore they were formed almost immediately after the big bang. None of these topological defects have so far been detected. It has been found that the density of magnetic monopoles today as predicted by the GUTs should be $n_M \approx 10^{-9} - 10^{-10} n_\gamma$ [43, 44], where n_γ is the photon density. Therefore, the magnetic monopole density should be roughly of the same order as the baryon density. However, searches for magnetic monopoles in seawater have shown that $n_M < 10^{-6}/\text{gram}$, corresponding roughly to $n_M < 10^{-30}/\text{nucleon}$ [45]. Searches for magnetic monopoles in the moon's wake have given the even more restrictive value of $n_M < 10^{-32}/\text{nucleon}$ [45]. Therefore, the prediction for the magnetic monopole density strongly disagrees with the observed value.

3 Inflation

Inflation is an epoch of accelerated expansion in the very early universe before the period of radiation domination. It can naturally be incorporated into the hot big bang model which postulates that the universe began in an infinitely hot and dense state followed by expansion and cooling. Inflation can solve the major cosmological problems discussed in section 2. In the following the evolution of the universe during this period of rapid expansion will be analysed using general relativity and scalar field theory.

In section 3.1 the basic single-field inflationary mechanism will be described. In section 3.2 this description will be used to explain how inflation can solve the cosmological problems of the standard hot big bang model. In section 3.3 the generation of scalar and tensor perturbations during a phase of accelerated expansion will be discussed and an overview of the non-gaussianity predicted by inflation will be given.

3.1 The Inflationary Universe

Inflation is a phase of accelerated expansion taking place shortly after the big bang during which the scale factor $a(t)$ increases nearly exponentially in time. Accelerated expansion corresponds to $\ddot{a} > 0$. The second Friedmann equation reads

$$\frac{\ddot{a}}{a} = -\frac{4\pi G}{3}(\rho + 3p). \quad (10)$$

Therefore, accelerated expansion requires a violation of the strong energy condition, so that $\rho + 3p < 0$. This condition can be realised using a simple field theoretical model in which inflation is driven by a classical scalar field ϕ that is slowly rolling down a positive, flat potential $V(\phi)$. This field is called the inflaton. The energy-momentum tensor for a classical scalar field is given by

$$T_{\beta}^{\alpha} = g^{\alpha\gamma}\phi_{,\gamma}\phi_{,\beta} - \delta_{\beta}^{\alpha}\left(\frac{1}{2}g^{\gamma\delta}\phi_{,\gamma}\phi_{,\delta} - V(\phi)\right). \quad (11)$$

Here, repeated indices are summed over. Unless explicitly stated otherwise this convention applies throughout the entire paper. It is assumed that the universe is a flat, homogeneous and isotropic Friedmann-Robertson-Walker universe, so that the metric is given by

$$ds^2 = g_{\mu\nu}dx^{\mu}dx^{\nu} = dt^2 - \delta_{ij}a^2(t)dx^i dx^j, \quad (12)$$

where $g_{\mu\nu}$ is the metric tensor. Assuming that the field is homogeneous, $\phi = \phi(t)$, and identifying $T_0^0 = \rho$ and $T_j^i = -\delta_j^i p$, one can find from (11) that the energy density ρ_ϕ and pressure p_ϕ of the scalar field are given by

$$\rho_\phi = \frac{1}{2}\dot{\phi}^2 + V(\phi), \quad (13)$$

$$p_\phi = \frac{1}{2}\dot{\phi}^2 - V(\phi). \quad (14)$$

Substituting this into the first Friedmann equation (1) and setting $k = 0$ one finds

$$H^2 = \frac{8\pi G}{3} \left(\frac{1}{2}\dot{\phi}^2 + V(\phi) \right). \quad (15)$$

By substituting the first Friedmann equation (1) and its time derivative into the second Friedmann equation (10) one can derive the energy conservation equation

$$\dot{\rho} = -3H(\rho + p). \quad (16)$$

Defining the equation of state parameter $w = p/\rho$ this can be integrated to give

$$\rho \propto a^{-3(1+w)}. \quad (17)$$

After substitution of the above expressions for ρ_ϕ and p_ϕ into (16) the energy conservation equation for the inflaton field is found to be

$$\ddot{\phi} + 3H\dot{\phi} + V_{,\phi} = 0, \quad (18)$$

where it has been used that $\dot{V} = V_{,\phi}\dot{\phi}$. The dynamical system given by (15) and (18) describes a homogeneous classical scalar field in an expanding background. This system leads to inflation if the field is rolling down the potential very slowly compared to the expansion of the universe. To ensure this, during inflation the potential $V(\phi)$ has to be very flat and much larger than the scalar field kinetic energy. The conditions for slow-roll of ϕ and $\dot{\phi}$ are given in (19) and (20), respectively

$$\frac{1}{2}\dot{\phi}^2 \ll |V(\phi)|, \quad (19)$$

$$|\ddot{\phi}| \ll 3H|\dot{\phi}|. \quad (20)$$

It can be seen that as long as (19) is fulfilled the equation of state parameter is close to $w_\phi \approx -1$. Thus, the slow-roll stage of inflation is characterised by $p_\phi \approx -\rho_\phi$ which does indeed correspond to accelerated expansion, as can be

seen from (10). Using (17) the first Friedmann equation (1) can be rewritten as

$$\frac{3H^2}{8\pi G} = \frac{c_m}{a^3} + \frac{c_r}{a^4} + \frac{c_\sigma}{a^6} + \dots + \frac{c_\phi}{a^{3(1+w_\phi)}} - \frac{k}{a^2}. \quad (21)$$

Here, the c_i are constants and the right-hand side of the equation gives the contributions to the energy density of (from left to right) matter, radiation, anisotropies, a scalar field component with equation of state w_ϕ and the curvature. It has just been shown that during inflation $w_\phi \approx -1$, such that the scalar field component in (21) is roughly constant. Since the scale factor $a(t)$ increases in time the term with the lowest power of the scale factor in the denominator will come to dominate the evolution of the universe. It can easily be seen that all components besides the inflaton field quickly decay, such that after a short amount of time the inflaton dominates the energy density and the universe inflates.

Using the slow-roll conditions (19),(20) the evolution equations given in (15) and (18) can be simplified to

$$H^2 \simeq \frac{8\pi G}{3} V(\phi), \quad (22)$$

$$3H\dot{\phi} \simeq -V_{,\phi}. \quad (23)$$

Using these expressions and their time derivatives the slow-roll conditions (19), (20) can be reformulated to give constraints on the shape of the potential

$$\frac{1}{6} \frac{1}{8\pi G} \left| \frac{V_{,\phi}}{V} \right|^2 \ll 1, \quad (24)$$

$$\frac{1}{3} \frac{1}{8\pi G} \left| \frac{V_{,\phi\phi}}{V} \right| \ll 1. \quad (25)$$

These slow-roll conditions are commonly given in terms of the two slow-roll parameters ϵ and δ , which are defined as

$$\epsilon = -\frac{\dot{H}}{H^2}, \quad \delta = \frac{\ddot{\phi}}{H\dot{\phi}}. \quad (26)$$

Then, during the slow-roll regime of inflation $|\epsilon| \ll 1$ and $|\delta| \ll 1$.

By integrating $H = \dot{a}/a$, using $dt = d\phi/\dot{\phi}$ and inserting equations (22) and (23) one can find the behaviour of the scale factor during slow-roll of the inflaton

$$a(t_2) \simeq a(t_1) \exp \left(\int_{\phi(t_2)}^{\phi(t_1)} 8\pi G \frac{V(\phi)}{V_{,\phi}(\phi)} d\phi \right). \quad (27)$$

The potential is positive and $V(\phi(t_1)) > V(\phi(t_2))$, therefore (27) corresponds to an exponential increase of the scale factor during inflation.

Inflation ends when the potential energy becomes smaller than the inflaton kinetic energy and the slow-roll conditions are no longer satisfied. The universe enters a stage of reheating. The inflaton field ϕ oscillates around the minimum of the potential $V(\phi)$ and its energy is converted into ordinary matter and radiation. The Standard Model particles produced interact with each other and thermal equilibrium is reached. The universe enters the well-known decelerating thermal Friedmann stage. For more details about reheating see e.g. [46].

3.2 Inflation and the Cosmological Problems

In section 2 some of the major problems of the hot big bang model have been introduced. In this section it will be shown how a period of accelerated expansion in the very early universe can solve these problems.

Flatness problem

In the standard decelerating big bang scenario the observed flatness of the universe today implies an extreme fine-tuning of the cosmological parameter $\Omega(t)$ at early times. This fine-tuning can be avoided by adding a sufficiently long period of inflation before the radiation dominated phase. Using (21) it has been shown in section 3.1 that as the universe expands the inflaton comes to dominate the evolution of the universe. The relative energy density of the curvature term decreases and the universe get closer and closer to being flat. This trend can be quantified as follows. During inflation the scale factor $a(t)$ increases roughly exponentially. In this approximation the Hubble parameter $H(t) = \dot{a}(t)/a(t)$ is constant. From (3) this implies that during the expansion the cosmological parameter decreases rapidly as $\Omega(t) - 1 \propto a^{-2}$. Therefore, $\Omega(t)$ is driven closer to unity during inflation. If from the beginning of inflation at time t_i until the end of inflation at time t_f the scale factor increases by a factor $e^N = e^{H(t_f - t_i)}$, this implies

$$\frac{\Omega(t_f) - 1}{\Omega(t_i) - 1} = \left(\frac{a(t_i)}{a(t_f)} \right)^2 = e^{-2N}. \quad (28)$$

One can assume that at the beginning of inflation $\Omega(t_i) - 1 \sim \mathcal{O}(1)$. While the exact value of $\Omega - 1$ at the end of inflation is unknown, it is definitely

larger than the corresponding value at the Planck time found in section 2. Therefore, the rough number of e-foldings the universe has to expand by during inflation can be found by approximating $\Omega(t_f) \approx \Omega(t_{pl})$. The resulting number of e-folds will more than suffice to solve the flatness problem. In this limit it is found from (28) that $e^{-2N} \approx 10^{-60}$. This implies that if inflation lasts a number of $N = 70$ e-foldings the value observed today $\Omega_0 = 1.02 \pm 0.02$ [42] is easily explained. For a larger value of N , $\Omega_0 = 1$ with even higher precision. Therefore, if inflation lasts sufficiently long the flatness problem is solved and the radiation dominated epoch of the standard big bang scenario naturally begins with locally negligible curvature.

Homogeneity/Horizon problem

The horizon problem is based on the observation that our universe is extremely homogeneous, even though it consists of many patches that were causally disconnected in the past. Inflation solves this problem. During inflation the Hubble radius $1/H(t)$ is roughly constant. The physical wavelength $a\lambda$ is rapidly growing and can thus leave the Hubble radius. This implies that the Hubble radius can be much smaller than the causally connected patch.

To quantify this one should recall the definition of the particle horizon (6). During inflation the scale factor grows exponentially with time $a(t) \propto e^{Ht}$. Inserting this into (6) and changing the lower integration limit to the beginning of inflation t_i , one can find that during inflation the particle horizon grows approximately by

$$d_p(t_f) = c \cdot a(t_f) \int_{t_i}^{t_f} \frac{dt}{a(t)} \approx \frac{c}{H} e^N. \quad (29)$$

In section 2 the ratio of the size of our homogeneous domain of the universe to the particle horizon size was investigated without considering inflation. As a rough approximation one can assume that without a period of inflation this ratio would be similar at time t_f and at the Planck time t_{pl} . We can then use the result found in (9). One can see from (29) that when taking into account inflation the value of the particle horizon at t_f is bigger than predicted in section 2, roughly by a factor of e^N . To solve the horizon problem, the ratio of the size of our homogeneous domain to the particle horizon has to be smaller than unity at time t_f . From (9) one can see that this is achieved if $e^N > 10^{30}$, corresponding to inflation lasting at least a number of e-folds $N \approx 70$. For this number of e-folds of inflation the observable universe has been in causal contact since the beginning of the radiation dominated epoch,

which explains the isotropy of the CMB and the homogeneity of our causal domain.

This approach included some strong approximations, so that only a rough estimate of N is obtained. However, this estimate agrees well with the values usually quoted in the literature [47, 48]. The above calculation clearly illustrates how inflation can explain the large-scale homogeneity of the observable universe by causing a rapid increase in the size of the particle horizon in the very early universe.

Origin of large-scale structure

One of the most important achievements of inflationary models is the production of density perturbations that can explain the deviation of the observed universe from a perfectly homogeneous flat Friedmann-Robertson-Walker model and can predict the observed large-scale structure. The inflation scenario described in section 3.1 generates gaussian scalar density perturbations with a nearly scale-invariant spectrum, as will be shown in the next section. These perturbations can lead to the formation of galaxies and explain the observed anisotropy in the cosmic microwave background. Inflation can also generate a spectrum of gravitational waves, leading to additional anisotropies in the microwave background.

In section 2 it was described how in a decelerating universe scales continuously enter the Hubble radius. The origin of these scales is unknown. Inflation manages to solve this problem in a very elegant manner. During the exponential expansion the Hubble length $1/H$ is roughly constant and the comoving Hubble length $1/aH$ is decreasing. The physical scales grow rapidly during inflation and can therefore leave the Hubble radius. The amplitudes of these modes become "frozen" at horizon crossing. After inflation ends the universe begins to decelerate and the Hubble radius grows. Scales start to re-enter the Hubble radius. Due to gravity these small perturbations grow over time and eventually become the structures that are observed today. Therefore, given a method of generation of small density perturbations during inflation, the structure formation problem is solved.

During inflation small perturbations can be generated at the quantum level. While inflation generally "washes out" inhomogeneities, due to the uncertainty principle the fields still undergo quantum fluctuations. These quantum fluctuations will always be present. During inflation the physical wavelengths

of these fluctuations increase exponentially. They are stretched beyond the quantum level and effectively become classical modes when leaving the horizon.

The explanation of the origin of large-scale structures is probably the most important achievement of inflationary theories. In this section only an intuitive argument has been given. The detailed calculation of the generation of density perturbations during inflation and the derivation of the resulting spectra will be given in section 3.3.

Monopole problem

One of the major cosmological problems is that, even though the magnetic monopole density is predicted to be of the same order as the baryon density, no magnetic monopoles have so far been observed. A similar problem applies to other exotic heavy particles and topological defects.

If a period of inflation took place after magnetic monopoles had been produced this problem can be solved. During a period of accelerated expansion particle densities decrease exponentially. Therefore, magnetic monopoles and other defects formed before inflation can exist today, but their densities are extremely low. This explains why these objects are so far undetected. Nucleons are created after inflation ends, so that their density is unaffected by inflation. Therefore, due to inflation the monopole to nucleon ratio strongly decreases. In section 2 it was stated that the measured magnetic monopole density is $n_M < 10^{-32}/\text{nucleon}$. To account for this upper bound on the monopole density, during inflation the horizon must have been extended by a factor of at least $e^N = n_M^{-1/3} \approx 10^{10}$, so that without inflation $n_M \approx \mathcal{O}(1)/\text{nucleon}$. This is solved by $N \geq 23$. Note that this is fulfilled anyway if the minimum requirement on the number of e-foldings to solve the flatness and horizon problems, $N \geq 70$, is satisfied.

Inflation could also take place before monopole production. Then a significant amount of monopoles could be produced during reheating when the inflaton energy is transferred to radiation and particles. However, if the reheating temperature is significantly lower than the monopole mass, then magnetic monopole production is avoided altogether, explaining why no monopoles are observed today.

3.3 Generation of Cosmological Perturbations

In this section the origin of the large-scale structure observed in the universe today will be discussed. First the generation of scalar perturbations during inflation will be analysed. Since we are dealing with small perturbations calculations to linear order in the perturbations will suffice. This will lead to a gaussian nearly scale-invariant spectrum of scalar perturbations. Afterwards non-gaussian corrections to this spectrum will briefly be discussed. Finally, tensor perturbations will be analysed and the almost scale-invariant gravitational wave spectrum predicted by inflation will be calculated.

Scalar perturbations

The metric of the homogeneous and isotropic background considered here corresponds to the metric of a flat, homogeneous and isotropic Friedmann-Robertson-Walker universe. It is given in (12). It will be useful to write this metric in terms of the conformal time τ , defined as

$$\tau = \int \frac{dt}{a(t)}. \quad (30)$$

Most of the following calculations will be carried out using conformal time τ instead of the cosmic time t . The background metric (12) can then be written as

$$ds^2 = a^2(\tau)(d\tau^2 - \delta_{ij}dx^i dx^j). \quad (31)$$

We would like to investigate this background metric with small perturbations superposed on it. There are three kinds of perturbations. Scalar perturbations are probably the most important type, since they are responsible for the large-scale structure of the universe. Vector perturbations are not as interesting in the inflationary picture, since they decay very quickly. They will not be discussed in this review. The last type are tensor perturbations, corresponding to gravitational waves. To linear order these three types of perturbations are uncoupled and can be dealt with one by one. This section is devoted to the analysis of scalar perturbations.

We want to analyse small perturbations to linear order in an otherwise homogeneous and isotropic, flat Friedmann-Robertson-Walker universe. The metric $g_{\mu\nu}$ for this analysis is given by the unperturbed background metric $g_{\mu\nu}^{(0)}$ given in (31) and a small metric perturbation $\delta g_{\mu\nu}$

$$g_{\mu\nu} = g_{\mu\nu}^{(0)} + \delta g_{\mu\nu}. \quad (32)$$

The most general line element for investigation of the scalar metric perturbations is given by [49, 50, 51]

$$ds^2 = a^2(\tau)((1 + 2A)d\tau^2 + 2B_{,i}d\tau dx^i - ((1 - 2\psi)\delta_{ij} - 2E_{,ij})dx^i dx^j). \quad (33)$$

It can be seen that four different scalar functions A , B , ψ , E show up in the perturbed metric, all of which are functions of the space and time coordinates. There is some gauge freedom in these quantities, as can be seen by investigating the change of the metric $g_{\mu\nu}$ under a coordinate transformation

$$x^\mu \rightarrow x'^\mu = x^\mu + \delta x^\mu. \quad (34)$$

Under such a transformation the metric tensor changes as

$$g'_{\mu\nu}(x'^\sigma) = \frac{\partial x^\alpha}{\partial x'^\mu} \frac{\partial x^\beta}{\partial x'^\nu} g_{\alpha\beta}(x^\sigma). \quad (35)$$

Inserting (32) and Taylor expanding $g_{\mu\nu}^{(0)}(x^\sigma + \delta x^\sigma)$ around x^σ , to first order the metric perturbations transform as

$$\delta g'_{\mu\nu} = \delta g_{\mu\nu} - g_{\mu\nu,\alpha}^{(0)} \delta x^\alpha - g_{\alpha\nu}^{(0)} \delta x_{,\mu}^\alpha - g_{\mu\alpha}^{(0)} \delta x_{,\nu}^\alpha. \quad (36)$$

Using this equation one can find the transformation properties of the scalar functions in the perturbed metric. One can decompose δx^i into a scalar ζ and a 3-vector v^i that has vanishing divergence, so that $\delta x^i = \partial^i \zeta + v^i$, with $v^i_{,i} = 0$. Using this decomposition under the coordinate transformation (34) the scalar functions transform as

$$\begin{aligned} A' &= A - \delta x^0_{,\tau} - \frac{a_{,\tau}}{a} \delta x^0, & B' &= B - \delta x^0 + \zeta_{,\tau}, \\ \psi' &= \psi + \frac{a_{,\tau}}{a} \delta x^0, & E' &= E + \zeta. \end{aligned} \quad (37)$$

It can be seen that only two scalar functions, δx^0 and ζ , contribute to this gauge transformation. Therefore, among the four scalar functions A, B, ψ, E there are two redundant degrees of freedom that can be removed without affecting the physics. Two gauge invariant quantities that will be useful in the following calculations are the two potentials

$$\Phi = A - \frac{1}{a}(a(B - E_{,\tau}))_{,\tau}, \quad \Psi = \psi + \mathcal{H}(B - E_{,\tau}). \quad (38)$$

Here, in analogy to the Hubble parameter $H(t)$ for cosmological time, $\mathcal{H}(\tau) = a_{,\tau}(\tau)/a(\tau)$ has been introduced. The invariance of the two potentials under coordinate transformations (34) can easily be verified using (37). To simplify

the following calculations we can eliminate the two redundant degrees of freedom by fixing the gauge. Our choice of gauge is given by the conditions $B = E = 0$. This is known as the longitudinal gauge. From (38) this implies that $\Phi = A$ and $\Psi = \psi$.

In addition to the metric perturbations, the scalar field driving inflation is also perturbed. This perturbation in the matter component leads to a perturbation of the energy-momentum tensor given in (11). The perturbations of the geometry and the matter are related by the perturbed Einstein equations

$$\delta G_\nu^\mu = 8\pi G \delta T_\nu^\mu. \quad (39)$$

δG_ν^μ is the perturbed Einstein tensor which can be calculated from the metric perturbations discussed above. This is a lengthy calculation which will be omitted here. The details of this calculation are for example given in [48]. The perturbed Einstein equations in the longitudinal gauge read

$$8\pi G \delta T_0^0 = \frac{2}{a^2} (\nabla^2 \Psi - 3\mathcal{H}(\mathcal{H}\Phi + \Psi_{,\tau})), \quad (40)$$

$$8\pi G \delta T_i^0 = \frac{2}{a^2} (\mathcal{H}\Phi + \Psi_{,\tau})_{,i}, \quad (41)$$

$$-8\pi G \delta T_{j=i}^i = \frac{1}{a^2} (2\Psi_{,\tau\tau} - \nabla^2(\Psi - \Phi) + 2\mathcal{H}(2\Psi_{,\tau} + \Phi_{,\tau}) + (4\mathcal{H}_{,\tau} + 2\mathcal{H}^2)\Phi), \quad (42)$$

$$-8\pi G \delta T_{j\neq i}^i = \frac{1}{a^2} (\Psi - \Phi)_{,ij}. \quad (43)$$

The first equation corresponds to (39) with $\mu = \nu = 0$, the second equation to $\mu = 0$ and $\nu = i$, the third equation comes from the $\mu = \nu = i$ component and the last equation corresponds to $\mu = i$ and $\nu = j$ with $i \neq j$. To further study these equations the perturbation of the matter component to first order has to be found. One can use the expression for the energy momentum tensor in (11) and the perturbed Friedmann-Robertson-Walker metric (33). The scalar field can be written as $\phi = \phi^{(0)} + \delta\phi$, where $\phi^{(0)}$ depends only on time and $\delta\phi$ is a scalar field perturbation that depends on all the spacetime coordinates. The perturbed components of the energy-momentum tensor then read

$$\begin{aligned} \delta T_0^0 &= \frac{1}{a^2} (\phi_{,\tau}^{(0)} \delta\phi_{,\tau} - A\phi_{,\tau}^{(0)2} + a^2 V_{,\phi} \delta\phi), & \delta T_i^0 &= \frac{1}{a^2} \phi_{,\tau}^{(0)} \delta\phi_{,i}, \\ \delta T_{j=i}^i &= \frac{1}{a^2} (-\phi_{,\tau}^{(0)} \delta\phi_{,\tau} + A\phi_{,\tau}^{(0)2} + a^2 V_{,\phi} \delta\phi), & \delta T_{j\neq i}^i &= 0. \end{aligned} \quad (44)$$

After inserting these expressions into the Einstein equations in (40) - (43) one can immediately see from (43) that $(\Psi - \Phi)_{,ij} = 0$, so that $\Psi = \Phi$.

Substituting this into (40) - (43), the Einstein equations read

$$\nabla^2\Phi - 3\mathcal{H}(\mathcal{H}\Phi + \dot{\Phi}) = 4\pi G(\phi_{,\tau}^{(0)}\delta\phi_{,\tau} - A\phi_{,\tau}^{(0)2} + a^2V_{,\phi}\delta\phi), \quad (45)$$

$$\mathcal{H}\Phi + \dot{\Phi} = 4\pi G\phi_{,\tau}^{(0)}\delta\phi, \quad (46)$$

$$\Phi_{,\tau\tau} + 3\mathcal{H}\dot{\Phi} + (2\mathcal{H}_{,\tau} + \mathcal{H}^2)\Phi = 4\pi G(\phi_{,\tau}^{(0)}\delta\phi_{,\tau} - A\phi_{,\tau}^{(0)2} - a^2V_{,\phi}\delta\phi). \quad (47)$$

An important quantity to study the perturbations generated during inflation is the intrinsic curvature perturbation on comoving hypersurfaces \mathcal{R} , defined as

$$\mathcal{R} = -\psi - \frac{H}{\dot{\phi}}\delta\phi. \quad (48)$$

This quantity can be rewritten in terms of the potential Φ using the Friedmann equations and the Einstein equation (46). It then reads

$$\mathcal{R} = -\Phi + \frac{H}{\dot{H}}(H\dot{\Phi} + \ddot{\Phi}). \quad (49)$$

It can be seen that the intrinsic curvature perturbation \mathcal{R} can be given entirely in terms of gauge-invariant quantities. Therefore, it is also gauge invariant. \mathcal{R} is a very important quantity, because outside the horizon it is constant on each scale for single-field inflation. This implies that its spectrum gives the curvature perturbation amplitude of different modes when they cross into the Hubble radius during the matter or radiation dominated epoch. \mathcal{R} can be expanded in Fourier space as

$$\mathcal{R} = \int \frac{d^3\mathbf{k}}{(2\pi)^{\frac{3}{2}}} \mathcal{R}_{\mathbf{k}}(\tau) e^{i\mathbf{k}\mathbf{x}}. \quad (50)$$

The power spectrum of the comoving curvature perturbation $P_{\mathcal{R}}(k)$ can then be defined using the vacuum expectation value

$$\langle \mathcal{R}_{\mathbf{k}} \mathcal{R}_{\mathbf{k}'}^* \rangle = \frac{2\pi^2}{k^3} P_{\mathcal{R}}(k) \delta^3(\mathbf{k} - \mathbf{k}'). \quad (51)$$

It should be noted that the power spectrum $P_{\mathcal{R}}(k)$ depends only on the magnitude of the wavenumber $|\mathbf{k}| \equiv k$.

In order to develop a correct understanding of the origin of perturbations in the early universe one needs to quantize the perturbations. The effective action during inflation is given by the sum of the actions for the gravitational field and the scalar field. The equations of motion for linear scalar perturbations can be derived from the action expanded up to second order in the

perturbations. After a partial integration the action for a perturbed inflaton field in a perturbed geometry is given by [49]

$$S = \int d^4x \mathcal{L} = \frac{1}{2} \int d^3\mathbf{x} d\tau \left((v_{,\tau})^2 - (v_{,i})^2 + \frac{z_{,\tau\tau}}{z} v^2 \right). \quad (52)$$

Here, two new variables have been introduced. The variable v which is related to the comoving curvature perturbation as

$$v \equiv -z\mathcal{R} = a \left(\delta\phi + \frac{\phi_{,\tau}}{\mathcal{H}} \psi \right) \quad (53)$$

and the function z , defined as

$$z \equiv a \frac{\phi_{,\tau}}{\mathcal{H}}. \quad (54)$$

It can be seen that the evolution of the perturbations can be investigated using a single variable v . The corresponding action (52) is of the same form as the action for a scalar field in Minkowski spacetime that has a time-dependent effective mass $m_{eff}^2 = -z_{,\tau\tau}/z$.

The canonical momentum $\pi_v(\tau, \mathbf{x})$ to the variable $v(\tau, \mathbf{x})$ can be calculated from the action (52) and is found to be

$$\pi_v(\tau, \mathbf{x}) = \frac{\partial \mathcal{L}}{\partial v_{,\tau}} = v_{,\tau}(\tau, \mathbf{x}). \quad (55)$$

The first step for quantization of the theory is the promotion of $v(\tau, \mathbf{x})$ and $\pi_v(\tau, \mathbf{x})$ to operators $\hat{v}(\tau, \mathbf{x})$ and $\hat{\pi}(\tau, \mathbf{x})$. One can then impose the standard quantum field theory equal time commutation relations on these two operators

$$\begin{aligned} [\hat{v}(\tau, \mathbf{x}), \hat{\pi}_v(\tau, \mathbf{x}')] &= i\delta^3(\mathbf{x} - \mathbf{x}'), \\ [\hat{v}(\tau, \mathbf{x}), \hat{v}(\tau, \mathbf{x}')] &= [\hat{\pi}_v(\tau, \mathbf{x}), \hat{\pi}_v(\tau, \mathbf{x}')] = 0. \end{aligned} \quad (56)$$

The operator $\hat{v}(\tau, \mathbf{x})$ can be expanded in Fourier space and then takes the form

$$\hat{v}(\tau, \mathbf{x}) = \int \frac{d^3\mathbf{k}}{(2\pi)^{\frac{3}{2}}} \left(v_k \hat{a}_{\mathbf{k}} e^{i\mathbf{k}\mathbf{x}} + v_k^* \hat{a}_{\mathbf{k}}^\dagger e^{-i\mathbf{k}\mathbf{x}} \right), \quad (57)$$

where $v_k = v_k(\tau)$ are complex and time-dependent coefficients. The operators $\hat{a}_{\mathbf{k}}$ and $\hat{a}_{\mathbf{k}}^\dagger$ are the creation and annihilation operators that are known from quantum theory. They satisfy the bosonic commutation relations

$$\left[\hat{a}_{\mathbf{k}}, \hat{a}_{\mathbf{k}'}^\dagger \right] = \delta^3(\mathbf{k} - \mathbf{k}'), \quad \left[\hat{a}_{\mathbf{k}}, \hat{a}_{\mathbf{k}'} \right] = \left[\hat{a}_{\mathbf{k}}^\dagger, \hat{a}_{\mathbf{k}'}^\dagger \right] = 0. \quad (58)$$

Substituting the expression for $\hat{v}(\tau, \mathbf{x})$ given in (57) and the corresponding easily derivable expression for $\hat{\pi}_v(\tau, \mathbf{x})$ into the equal time commutation relations (56) and using the bosonic commutation relations (58) one can find the normalization condition for the coefficients $v_k(\tau)$

$$v_k^* v_{k,\tau} - v_k v_{k,\tau}^* = -i. \quad (59)$$

The quantization of the theory also requires the definition of the vacuum state $|0\rangle$. Here it is defined by the condition

$$\hat{a}_{\mathbf{k}}|0\rangle = 0, \quad (60)$$

i.e. the vacuum state is the state that is annihilated by all $a_{\mathbf{k}}$. Other choices for the vacuum state are possible, but this is the most natural choice.

By varying the action (52) with respect to v and then requiring this variation to be zero the equation of motion for the functions v_k can be found. In Fourier space this equation of motion reads

$$v_{k,\tau\tau} + \left(k^2 - \frac{z_{,\tau\tau}}{z}\right)v_k = 0. \quad (61)$$

On small scales well inside the horizon, corresponding to $k/aH \rightarrow \infty$, the influence of the spacetime curvature on the mode behaviour is negligible. Therefore, these modes behave as if they were in the usual Minkowski vacuum and v_k approaches a plane wave form in the small wavelength limit

$$v_k \Big|_{\frac{k}{aH} \rightarrow \infty} \rightarrow \frac{1}{\sqrt{2k}} e^{-ik\tau}. \quad (62)$$

For modes in the long wavelength regime, corresponding to $k/aH \rightarrow 0$, $k^2 \ll z_{,\tau\tau}/z$ and the equation of motion (61) reduces to

$$v_{k,\tau\tau} \approx \frac{z_{,\tau\tau}}{z} v_k, \quad (63)$$

so that the solution $v_k \propto z$ is found. For further attempts to solve the equation of motion it should be noted that an explicit expression for $z_{,\tau\tau}/z$ can be found in terms of the slow-roll parameters defined in (26). It is given by

$$\frac{z_{,\tau\tau}}{z} = \frac{a\dot{a}\dot{z} + a^2\ddot{z}}{z} = \dot{a}^2 \left(2 + 2\epsilon + 3\delta + \epsilon\delta + \delta^2 + \frac{\dot{\epsilon}}{H} + \frac{\dot{\delta}}{H} \right). \quad (64)$$

Now it is time to return to the quantity of interest, the power spectrum of the comoving curvature perturbation $P_{\mathcal{R}}(k)$. After promoting the comoving

curvature perturbation \mathcal{R} to an operator $\hat{\mathcal{R}}$ and using the Fourier expansions of $\hat{\mathcal{R}}$ and \hat{v} given in (50) and (57) the expectation value $\langle 0|\hat{\mathcal{R}}_k\hat{\mathcal{R}}_{k'}^\dagger|0\rangle$ can be found. One should use the operator version of (53) to related $\hat{\mathcal{R}}$ and \hat{v} and make use of the vacuum state annihilation (60). Assuming that the vacuum state is normalized $\langle 0|0\rangle = 1$ the power spectrum defined in (51) is found to be

$$P_{\mathcal{R}}(k) = \frac{k^3}{2\pi^2} \frac{|v_k|^2}{z^2}. \quad (65)$$

To get an idea of the shape of this power spectrum the system described above will be investigated in the slow-roll regime. The equation of motion (61) can be solved in the limit that the two slow-roll parameters ϵ and δ given in (26) are constant. Assuming also that $\epsilon < 1$, the conformal time τ defined in (30) is approximately given by

$$\tau \approx -\frac{1}{(1-\epsilon)aH}. \quad (66)$$

For constant slow-roll parameters the derivatives in (64) can be neglected and in this limit

$$\frac{z_{,\tau\tau}}{z} = \frac{\nu_{\mathcal{R}}^2 - \frac{1}{4}}{\tau^2}, \quad (67)$$

where $\nu_{\mathcal{R}}$ is given by

$$\nu_{\mathcal{R}} = \frac{1}{2} + \frac{1+\epsilon+\delta}{1-\epsilon}. \quad (68)$$

The equation of motion in (61) then reads

$$v_{k,\tau\tau} + \left(k^2 - \frac{\nu_{\mathcal{R}}^2 - \frac{1}{4}}{\tau^2}\right)v_k = 0. \quad (69)$$

For $\nu_{\mathcal{R}}$ a real number the general solution to this equation is a linear combination of the Hankel functions of first and second kind

$$v_k = \sqrt{|\tau|}(c_1(k)H_{\nu_{\mathcal{R}}}^{(1)}(k|\tau|) + c_2(k)H_{\nu_{\mathcal{R}}}^{(2)}(k|\tau|)), \quad (70)$$

where $H_{\nu_{\mathcal{R}}}^{(1)}$ is the Hankel function of first kind of order $\nu_{\mathcal{R}}$ and correspondingly $H_{\nu_{\mathcal{R}}}^{(2)}$ is the Hankel function of second kind of order $\nu_{\mathcal{R}}$. In the asymptotic past, $k\tau \rightarrow -\infty$, (70) should reflect the Minkowski vacuum state given in (62). This asymptotic behaviour at small scales together with the correct normalisation can be achieved by setting $c_2(k) = 0$ and $c_1(k) = \frac{\sqrt{\pi}}{2}e^{i(\nu_{\mathcal{R}}+\frac{1}{2})\frac{\pi}{2}}$. The resulting expression for v_k with the appropriate behaviour in the asymptotic past is then

$$v_k = \frac{\sqrt{\pi|\tau|}}{2}e^{i(\nu_{\mathcal{R}}+\frac{1}{2})\frac{\pi}{2}}H_{\nu_{\mathcal{R}}}^{(1)}(k|\tau|). \quad (71)$$

For small, real arguments $x \ll 1$ the Hankel function of first kind $H_{\nu_{\mathcal{R}}}^{(1)}(x)$ can be approximated by

$$H_{\nu_{\mathcal{R}}}^{(1)}(x) \rightarrow \frac{-i}{\pi} \Gamma(\nu_{\mathcal{R}}) \left(\frac{x}{2}\right)^{-\nu_{\mathcal{R}}}. \quad (72)$$

Noting that the large scale limit $k/aH \rightarrow 0$ corresponds to small $k|\tau|$, this approximation can be used in (71), so that the expression for v_k becomes

$$v_k \rightarrow \frac{e^{i(\nu_{\mathcal{R}} - \frac{1}{2})\frac{\pi}{2}} \Gamma(\nu_{\mathcal{R}})}{\sqrt{2k} \Gamma(\frac{3}{2})} 2^{\nu_{\mathcal{R}} - \frac{3}{2}} (k|\tau|)^{\frac{1}{2} - \nu_{\mathcal{R}}}, \quad (73)$$

where it has been used that $\sqrt{\pi}/2 = \Gamma(3/2)$. This expression can be inserted in (65) and, after using (54) and (66), gives an expression for the power spectrum

$$P_{\mathcal{R}}^{\frac{1}{2}}(k) = \frac{\Gamma(\nu_{\mathcal{R}})}{\Gamma(\frac{3}{2})} (1 - \epsilon) \frac{H^2}{2\pi|\dot{\phi}|} \left(\frac{k|\tau|}{2}\right)^{\frac{3}{2} - \nu_{\mathcal{R}}}. \quad (74)$$

To characterise the scale dependence of this power spectrum the spectral index of the comoving curvature perturbation n_S can be used. It is obtained from the logarithmic momentum derivative of the scalar power spectrum

$$n_S - 1 = \frac{d \ln P_{\mathcal{R}}}{d \ln k}. \quad (75)$$

An exactly scale-invariant spectrum of curvature perturbations corresponds to a scalar spectral index of $n_S = 1$. A spectral index $n_S > 1$ corresponds to a blue-tilted spectrum and if $n_S < 1$ the spectrum is red-tilted. One can calculate the scalar spectral index to first order in the slow-roll parameters by noting that to first order $\nu_{\mathcal{R}} \approx \frac{3}{2} + 2\epsilon + \delta$. In this approximation the scalar spectral index is found to be

$$n_S \approx 1 - 4\epsilon - 2\delta. \quad (76)$$

Since during inflation the slow-roll parameters take very small values $|\epsilon|, |\delta| \ll 1$, one can see that the resulting spectrum of scalar perturbations is very close to being scale invariant. In fact, the chaotic inflation scenario discussed in section 3.1 predicts a slightly red-tilted, nearly scale-invariant spectrum of adiabatic perturbations, while other inflationary models can predict a blue-tilted spectrum [47]. An example for this would be the hybrid inflation model [52, 53], which relies on the presence of more than one scalar fields.

The above calculation has been carried out assuming that the slow-roll parameters ϵ and δ are small and time-independent. While this is only an approximation, the obtained results are in fact quite accurate, so that a very realistic expression for the scalar spectral index generated by single-field inflation was found.

Non-gaussianity

In the above calculation the spectrum of primordial scalar perturbations generated during single-field inflation has been discussed to linear order. To this order the spectrum is gaussian. While non-gaussian corrections to this spectrum do exist, their magnitude is very small. Therefore, a gaussian spectrum is a very good approximation. A thorough analysis of non-gaussianity in single-field inflationary models is beyond the scope of this paper. Only a brief description of the calculation procedure will be given and the final results for the amount of non-gaussianity that is generated will be stated. The discussion will focus on second-order non-gaussianity of the local form. For a detailed analysis of higher order corrections to the spectrum of scalar perturbations calculated to linear order in the perturbations one should see e.g. [54, 55, 56].

The reason why non-gaussianities produced during inflation are small can be understood using a simple intuitive argument. Density perturbations are created when the inflaton is slowly rolling down an almost constant potential $V(\phi)$, corresponding to an equation of state $w \approx -1$. Since the inflaton potential is very flat, the self-interaction terms of the scalar field are small and the inflaton behaves almost like a free field. In the perfect quantum limit a completely free field would generate perfectly gaussian quantum fluctuations, for which the two-point correlation function characterises the entire spectrum. Since the inflaton is not completely free, there are small non-gaussian corrections to this spectrum. Their amplitude depends on the exact value of the slow-roll parameter ϵ and thus on how close the potential is to being perfectly flat.

The amount of non-gaussianity generated during inflation can be found by extending the calculation of the spectrum of scalar perturbations given above to higher orders. One can expand the action (52) up to cubic order by taking into account non-linearities in the inflaton potential and in the Einstein action. The cubic interaction terms in the lagrangian lead to a non-linear evolution and can be used to compute the comoving curvature perturbation \mathcal{R} up to second order. One can then find the corresponding three-point function. This function vanishes for purely gaussian perturbations and thus provides information about the non-gaussianity in the density perturbation spectrum. Deviations from gaussianity can be characterised by the non-gaussianity parameter f_{NL} , whose meaning becomes apparent when writing

the comoving curvature perturbation as

$$\mathcal{R} = \mathcal{R}_0(1 + \frac{3}{5}f_{NL}\mathcal{R}_0). \quad (77)$$

Here, \mathcal{R}_0 is the gaussian linear curvature perturbation that was investigated above. The second term on the right corresponds to second-order corrections. These non-gaussian corrections are parameterised by f_{NL} . This parameter can be given in terms of the scalar spectral index as [55]

$$f_{NL} \approx \frac{5}{12}(n_s - 1) + f_k, \quad (78)$$

where f_k is a momentum-dependent function that is first-order in the slow-roll parameters. Since the scalar density perturbation spectrum is very close to being scale invariant and the slow-roll parameters are much smaller than unity, the value of f_{NL} predicted by inflation is very small. One can also see that the higher the deviation from scale-invariance, the more important are the non-gaussianities. Usually in models of single-field inflation $|f_{NL}| \approx 1$ or smaller [54].

It should be noted that a much larger non-gaussian signature can be generated in more complicated inflationary scenarios that include several fields [57, 58] or complex kinetic terms [59].

Tensor perturbations

In addition to scalar perturbations inflation also generates a nearly scale-invariant spectrum of tensor perturbations that could soon be observed as primordial gravitational waves. Like the scalar perturbations, tensor perturbations originate from vacuum quantum fluctuations. The procedure to calculate the spectrum of gravitational waves is almost the same as the calculation of the scalar perturbation spectrum, so that some steps of the calculation will not have to be repeated here.

The line element corresponding to a flat Friedmann-Robertson-Walker background with linear tensor perturbations reads [50, 51]

$$ds^2 = a^2(\tau)(d\tau^2 - (\delta_{ij} - h_{ij})dx^i dx^j). \quad (79)$$

The tensor perturbations h_{ij} are symmetric and satisfy $\delta^{ij}h_{ij} = 0$ and $h_{ij,i} = 0$, so that h_{ij} is traceless and transverse. Also, the 3-tensor h_{ij} does not transform under the coordinate transformation (34) and therefore the quantity is

gauge-invariant. Counting the number of degrees of freedom it is found that the gravitational waves have two independent polarization states $\lambda = 1, 2$.

To find the equation of motion and calculate the perturbation spectrum the action expanded up to second order in the perturbations has to be used. It contains the tensor part [49]

$$S_T = \frac{1}{64\pi G} \int d^3\mathbf{x} d\tau a^2(\tau) \eta^{\mu\nu} \partial_\mu h_j^i \partial_\nu h_i^j, \quad (80)$$

where $\eta^{\mu\nu} = \text{diag}(1, -1, -1, -1)$ is the Minkowski metric. This action can be written in a simpler way by setting $D_j^i = (1/\sqrt{32\pi G})h_j^i$ to get rid of the prefactor. D_j^i can then be expanded in Fourier space

$$D_j^i = \int \frac{d^3\mathbf{k}}{(2\pi)^{\frac{3}{2}}} \sum_{\lambda=1}^2 \varphi_{\mathbf{k},\lambda} \epsilon_j^i(\mathbf{k}, \lambda) e^{i\mathbf{k}\mathbf{x}}, \quad (81)$$

where $\varphi_{\mathbf{k},\lambda} = \varphi_{\mathbf{k},\lambda}(\tau)$ are complex and time-dependent coefficients and $\epsilon_j^i(\mathbf{k}, \lambda)$ is the time-independent polarization tensor. This tensor naturally satisfies the same conditions as the tensor perturbations h_{ij} , so that it is symmetric and $\delta^{ij} \epsilon_{ij} = k^i \epsilon_{ij} = 0$. Additionally $\epsilon_j^i(\mathbf{k}, \lambda) \epsilon_i^{j*}(\mathbf{k}, \sigma) = \delta_{\lambda\sigma}$. To simplify the following calculations it will be convenient to choose $\epsilon_{ij}^*(\mathbf{k}, \lambda) = \epsilon_{ij}(-\mathbf{k}, \lambda)$. One can define the new variable

$$v_{\mathbf{k},\lambda} = a\varphi_{\mathbf{k},\lambda}. \quad (82)$$

Using the properties of the polarization tensor given above and the Fourier expansion of D_j^i in (81) it can be seen that $v_{-\mathbf{k},\lambda} = v_{\mathbf{k},\lambda}^*$. After a partial integration and neglecting a total derivative the action (80) can be rewritten in terms of the variable $v_{\mathbf{k},\lambda}$. It then reads

$$S = \frac{1}{2} \int d\tau d^3\mathbf{k} \sum_{\lambda=1}^2 \left(\left| \frac{d^2 v_{\mathbf{k},\lambda}}{d\tau^2} \right|^2 - \left(k^2 - \frac{a_{,\tau\tau}}{a} \right) |v_{\mathbf{k},\lambda}|^2 \right). \quad (83)$$

As was done in the analysis of scalar perturbations the theory now has to be quantized. The variable $v_{\mathbf{k},\lambda}(\tau)$ is promoted to an operator $\hat{v}_{\mathbf{k},\lambda}(\tau)$. This operator can be written in terms of the scalar modes $v_k(\tau)$ that have been used when quantizing the scalar perturbations, and the creation and annihilation operators $\hat{a}_{\mathbf{k},\lambda}, \hat{a}_{\mathbf{k},\lambda}^\dagger$

$$\hat{v}_{\mathbf{k},\lambda} = v_k \hat{a}_{\mathbf{k},\lambda} + v_k^* \hat{a}_{\mathbf{k},\lambda}^\dagger. \quad (84)$$

The creation and annihilation operators satisfy the usual commutation relations

$$\left[\hat{a}_{\mathbf{k},\lambda}, \hat{a}_{\mathbf{k}',\sigma}^\dagger \right] = \delta^3(\mathbf{k} - \mathbf{k}') \delta_{\lambda\sigma}, \quad \left[\hat{a}_{\mathbf{k},\lambda}, \hat{a}_{\mathbf{k}',\sigma} \right] = \left[\hat{a}_{\mathbf{k},\lambda}^\dagger, \hat{a}_{\mathbf{k}',\sigma}^\dagger \right] = 0. \quad (85)$$

Again the vacuum state $|0\rangle$ is defined as the state that is annihilated by the annihilation operator $\hat{a}_{\mathbf{k},\lambda}|0\rangle = 0$.

The equation of motion for $v_k(\tau)$ can be derived by varying the action given in (80). It is found to be

$$v_{k,\tau\tau} + \left(k^2 - \frac{a_{,\tau\tau}}{a} \right) v_k = 0. \quad (86)$$

This is very similar to the equation of motion for the scalar perturbations given in (61). The only difference is that the factor $z_{,\tau\tau}/z$ is replaced by $a_{,\tau\tau}/a$. Exploiting this similarity the behaviour of v_k on small scales and large scales can immediately be found

$$v_k \Big|_{\frac{k}{aH} \rightarrow \infty} \rightarrow \frac{1}{\sqrt{2k}} e^{-ik\tau}, \quad v_k \Big|_{\frac{k}{aH} \rightarrow 0} \propto a. \quad (87)$$

To solve the equation of motion (86) a similar strategy as used for the analysis of scalar perturbations can be applied. One should note that

$$\frac{a_{,\tau\tau}}{a} = \dot{a}^2 + \ddot{a}a = (aH)^2(2 - \epsilon). \quad (88)$$

In the approximation that the slow-roll parameter ϵ is constant the conformal time is given by (66), so that (88) can be approximated as

$$\frac{a_{,\tau\tau}}{a} = \frac{(\nu_T^2 - \frac{1}{4})}{\tau^2}. \quad (89)$$

Here, ν_T gives the dependence on the slow-roll parameter ϵ

$$\nu_T = \frac{1}{2} + \frac{1}{1 - \epsilon}. \quad (90)$$

The equation of motion for v_k then reads

$$v_{k,\tau\tau} + \left(k^2 - \frac{(\nu_T^2 - \frac{1}{4})}{\tau^2} \right) v_k = 0. \quad (91)$$

The power spectrum for gravitational waves $P_T(k)$ can be defined using the vacuum expectation value

$$32\pi G \cdot \langle 0 | \hat{\varphi}_{\mathbf{k},\lambda} \hat{\varphi}_{\mathbf{k}',\lambda}^\dagger | 0 \rangle = \frac{2\pi^2}{k^3} P_T(k) \delta^3(\mathbf{k} - \mathbf{k}'). \quad (92)$$

The gravitational wave power spectrum results from the tensor perturbations h_{ij} and not from the rescaled variable $D_{ij} = h_{ij}/\sqrt{32\pi G}$ with Fourier coefficients $\varphi_{\mathbf{k},\lambda}$. This explains the origin of the prefactor of $32\pi G$. Using the definition of the vacuum state $\hat{a}_{\mathbf{k},\lambda}|0\rangle = 0$ and the expansion of $\hat{v}_{\mathbf{k},\lambda} = a\hat{\varphi}_{\mathbf{k},\lambda}$ in creation and annihilation operators (84) one can find

$$\langle 0|\hat{\varphi}_{\mathbf{k},\lambda}\hat{\varphi}_{\mathbf{k}',\lambda}^\dagger|0\rangle = 2\frac{|v_k|^2}{a^2}\delta^3(\mathbf{k} - \mathbf{k}'), \quad (93)$$

where the factor 2 comes from the fact that there are two possible polarization states $\lambda = 1, 2$.

One should note that the equation of motion (91) has exactly the same form as the equation of motion (69) found when calculating the spectrum of scalar perturbations, with $\nu_{\mathcal{R}}$ replaced by ν_T . Following the exact same procedure as in the analysis of the scalar perturbations the tensor power spectrum can be obtained and is given by

$$P_T^{\frac{1}{2}}(k) = \sqrt{32\pi G} \cdot 2^{\nu_T-1} \frac{\Gamma(\nu_T)}{\Gamma(\frac{3}{2})} (1-\epsilon) \frac{H}{2\pi} (k|\tau|)^{\frac{3}{2}-\nu_T}. \quad (94)$$

The spectral index of tensor perturbations n_T is defined as

$$n_T = \frac{d\ln P_T}{d\ln k}. \quad (95)$$

From the expression for the tensor power spectrum given in (94) one can find

$$n_T = 3 - 2\nu_T \approx -2\epsilon, \quad (96)$$

where the last expression is an approximation to lowest order in the slow-roll parameter ϵ . A scale-invariant spectrum corresponds to $n_T = 0$. Since during inflation ϵ is small, the predicted spectrum of gravitational waves is close to scale-invariant. Since $\epsilon > 0$ in inflationary models, $n_T < 0$, such that the predicted spectrum is tilted slightly to the red.

An important quantity is the tensor to scalar ratio r which is given by the ratio of the tensor power spectrum to the scalar power spectrum

$$r \equiv \frac{P_T}{P_{\mathcal{R}}}. \quad (97)$$

By inserting the expressions for the power spectra of curvature and tensor perturbations given in (74) and (94), respectively, and using the equations of motion during slow-roll inflation (22) and (23), as well as the definition

of the slow-roll parameter in (26), this ratio is approximately found to be $r \approx 16\epsilon$. One can easily relate this to the tensor spectral index given in (176) to find

$$r = -8n_T. \tag{98}$$

This is known as the consistency relation for single-field slow-roll inflation.

4 The Ekpyrotic/Cyclic Universe

The ekpyrotic model of the universe [21] is an attempt to solve all of the cosmological problems described in section 2 without relying on a period of inflation. Instead it includes a period of ultra-slow contraction, called the ekpyrotic phase, that occurs before the big bang. Due to this period the cosmological problems can be solved. The cyclic universe [29, 30] is an extension of the ekpyrotic model. It incorporates an ekpyrotic phase while also offering predictions concerning the far past and future of our universe. In the ekpyrotic and cyclic models the big bang is not the beginning of time. It is a physical event that is part of the history of the universe.

The ekpyrotic and cyclic models are strongly inspired by string and M-theory. They rely on the braneworld picture of the universe. This picture is based on five-dimensional heterotic M-theory [22, 23, 24, 25, 26], a unified theory of gravity and particle physics. It proposes the existence of two parallel boundary branes which contain the bulk spacetime between them. The bulk spacetime is five-dimensional, while the branes are (3+1)-dimensional and can be infinite in these dimensions. The fifth dimension is confined to a line segment whose endpoints are the two boundary branes. Since the theory is embedded in M-theory, each spacetime point is associated with six additional dimensions. Therefore, the scenario relies on an overall eleven-dimensional theory that consists of a ten-dimensional spacetime and a line segment.

One of the two boundary branes in the set-up corresponds to our universe. All matter and forces live on the branes. Only gravity is unbound and free to propagate in the bulk spacetime. Therefore, the only type of interaction between the two separated branes is gravitational. An attractive force, described by a scalar potential $V(\phi)$, acts between the branes. They approach each other along the fifth dimension and eventually collide. This slightly inelastic collision is identified with the hot big bang of standard cosmology and leads to matter and radiation being produced in the universe. After the collision the branes separate again. It should be noted that during the collision only the orbifold dimension becomes zero, while the other four dimensions are finite at the big bang. The effective four-dimensional scale factor does vanish, but the brane scale factors are finite at the collision, so that the big bang happens at finite temperature and density. Therefore, the big bang singularity is a very mild singularity [36]. While for a proper modelling of the behaviour of the universe at the singularity a theory of quantum gravity is needed, due to its mildness the understanding of the physics involved has

already significantly improved (see e.g. [60, 61, 62, 63, 36, 64]) and there is hope that this issue can be resolved in the near future.

While the higher-dimensional picture is important for a thorough understanding of the ekpyrotic model, almost all aspects of the scenario can be described using a four-dimensional low energy effective theory. The main aim of this paper is to describe an alternative cosmological model and its solutions to the cosmological problems in enough detail to contrast it with inflationary cosmology. To achieve this, investigating the four-dimensional effective description is sufficient and we will focus on this in the following. For details about the fundamental theory and the embedding of the effective theory in heterotic M-theory see e.g. [65, 66, 41] and references therein. In the four-dimensional theory the ekpyrotic universe can be analysed using general relativity and scalar field cosmology, similar to the analysis of inflation in section 3.

The cyclic universe is an important scenario based on the ekpyrotic model. It includes an ekpyrotic phase that solves the cosmological problems, while also explaining the existence of dark energy. It aims at providing a complete history of the universe. The cyclic model also relies on the braneworld picture inspired by heterotic M-theory and the set-up is exactly the same as described above. The main difference is that while the ekpyrotic scenario assumes only one brane collision, the cyclic universe predicts infinitely many. In the cyclic model after the branes bounce and separate, due to a spring-like force between the branes they eventually start attracting each other again. This force is very weak when the branes are far apart, but it increases as they approach each other. After a long time the branes are very close and the potential energy becomes negative, inducing a second ekpyrotic phase and ultimately a second brane collision. The process then repeats itself, resulting in a cyclic evolution of the universe. The small attractive force operating between the boundary branes is identified with the dark energy that is observed today. The cyclic model of the universe can also be described using an effective four-dimensional theory.

In section 4.1 the properties of the single-field ekpyrotic phase will be discussed. Afterwards, a detailed description of the cyclic universe will be given in section 4.2. In section 4.3 it will be explained how the ekpyrotic/cyclic universe manages to solve the major cosmological problems. An analysis of the generation of scalar and tensor perturbations, including a discussion of non-gaussianity, will be given in section 4.4. For the analysis of the scalar perturbations the scenario will be extended to include two scalar fields.

4.1 The Ekpyrotic Phase

The main prediction of the ekpyrotic model of the universe is the existence of an ekpyrotic phase preceding the big bang. The ekpyrotic phase is a period of slow contraction during which the scale factor is almost constant, while the Hubble radius is rapidly decreasing. Ekpyrosis requires an ultra-stiff equation of state $w \gg 1$. Using this ultra-slow contracting phase the ekpyrotic model can solve all of the cosmological problems described in section 2.

The ekpyrotic phase can be described using a scalar field ϕ rolling down a potential $V(\phi)$. The requirements on the potential can be found from the equation of state for the field. Using the average energy density ρ_ϕ and average pressure p_ϕ of a scalar field given in (13) and (14) respectively, one finds

$$w_\phi = \frac{p_\phi}{\rho_\phi} = \frac{\frac{1}{2}\dot{\phi}^2 - V(\phi)}{\frac{1}{2}\dot{\phi}^2 + V(\phi)}. \quad (99)$$

An equation of state $w_\phi > 1$ can thus only be fulfilled if the potential $V(\phi)$ is negative during the ekpyrotic phase. Another condition on the potential is that it must be very steep. Therefore, the ekpyrotic phase can be described by a scalar field rolling down a steep, negative potential. Considering the first Friedmann equation rewritten as in (21) one can see that in this scenario the scalar field comes to dominate the evolution of the universe. The universe is contracting during the ekpyrotic phase, so that the scale factor a decreases in time. Therefore, the term with the highest power of a in the denominator comes to dominate. In the absence of the scalar field this would be the anisotropy term c_σ/a^6 . The universe would become increasingly inhomogeneous which would lead to a state that is excluded by observations. In the presence of a scalar field with equation of state $w_\phi > 1$ the picture is different. In this case the power of the scale factor in the denominator of the corresponding term is $3(1 + w_\phi) > 6$, therefore the energy density in the scalar field starts to dominate during the ekpyrotic phase as $a \rightarrow 0$, while the relative energy densities of the anisotropy and other matter terms quickly decay.

The general ekpyrotic scenario can involve more than one scalar field. The action for N decoupled scalar fields ϕ_i , $i = 1, \dots, N$, with corresponding potentials $V_i(\phi_i)$, that interact only via gravity is given by

$$S = \int d^4x \sqrt{-g} \left(-\frac{R}{16\pi G} + \frac{1}{2} \sum_{i=1}^N \partial_\mu \phi_i \partial^\mu \phi_i - \sum_{i=1}^N V_i(\phi_i) \right), \quad (100)$$

where R is the Ricci scalar and g is the determinant of the metric tensor $g_{\mu\nu}$. The equations of motion for this action can easily be derived, using that each of the scalar fields has an energy density ρ_i given by (13). Choosing again as background a homogeneous and isotropic Friedmann-Robertson-Walker spacetime that is spatially flat, and neglecting the contribution of other matter components to the energy density, one finds from the first Friedmann equation (1) with $k = 0$

$$H^2 = \frac{8\pi G}{3} \left(\frac{1}{2} \sum_{i=1}^N \dot{\phi}_i^2 + \sum_{i=1}^N V_i(\phi_i) \right). \quad (101)$$

The equations describing the evolution of the scalar fields can be found from energy conservation (16) which is given independently for each field. They read

$$\ddot{\phi}_i + 3H\dot{\phi}_i + V_{i,\phi_i} = 0, \quad (102)$$

where $V_{i,\phi_i} \equiv \partial V_i / \partial \phi_i$, with no summation implied. Since most of the cosmological problems can be solved using single-field ekpyrosis, for simplicity we will focus on this case for now. We will return to the case of several scalar fields when discussing the origin of density perturbations. For a single scalar field the equations of motion reduce to the standard equations of single scalar field cosmology that have already been obtained in section 3 and are given in (15) and (18). In the higher dimensional theory the scalar field ϕ parameterises the distance between the two boundary branes. Its potential $V(\phi)$ represents the attractive force that leads to the branes approaching each other and ultimately causes the big crunch.

A simple choice for a steep, negative potential is a negative exponential

$$V(\phi) = -V_0 e^{-c\phi}, \quad (103)$$

where V_0 and c are positive constants. For this potential the equations of motion are solved by the scaling solution [67, 68]

$$a(t) \propto (-t)^p, \quad \phi(t) = \sqrt{\frac{p}{4\pi G}} \log \left(-\sqrt{\frac{8\pi G V_0}{(1-3p)p}} t \right), \quad p = \frac{16\pi G}{c^2}. \quad (104)$$

Using the time dependence of $a(t)$, the Hubble parameter $H(t)$ during ekpyrosis can be found. It is given by $H(t) = p/t$, so that during the ekpyrotic phase the Hubble radius is decreasing in time. Using this scaling solution and the expression for the potential (103) and inserting it into (99) the corresponding equation of state is found to be constant and is given by

$$w_\phi = \frac{2}{3p} - 1. \quad (105)$$

The time of the big crunch is commonly defined as $t = 0$, thus the time variable is negative and increasing during the ekpyrotic phase $t < 0$. Then, from the scaling solution (104) it can easily be seen that the scale factor decreases in time, which corresponds to a contracting universe. The condition for this contraction to be slow, and thus for $a(t) \propto (-t)^p$ to be slowly varying, is that p is very small $p \ll 1$. It can be seen from (105) that this condition leads to the desired equation of state $w_\phi \gg 1$. Therefore, in order to have a slowly contracting ekpyrotic phase it is required that

$$\bar{\epsilon} \equiv -\frac{\dot{H}}{H^2} = \frac{1}{p} \gg 1, \quad (106)$$

where the fast-roll parameter $\bar{\epsilon}$ has been defined. This parameter leads to constraints on the steepness of the ekpyrotic potential $V(\phi)$. Using the scaling solution (104) and the expression for the potential (103) two conditions on the potential to ensure fast-roll can be derived

$$\frac{1}{16\pi G} \left| \frac{V_{,\phi}}{V} \right|^2 \gg 1, \quad (107)$$

$$\frac{1}{16\pi G} \left| \frac{V_{,\phi\phi}}{V} \right| \gg 1. \quad (108)$$

4.2 The Cyclic Universe

The cyclic universe is a cosmological model which postulates that the universe is undergoing an endless sequence of expansion and contraction, while also incorporating a period of dark energy domination in the cycle. It is based on the ekpyrotic scenario, so that the evolution of the universe can be described using a scalar field ϕ moving along its effective potential $V(\phi)$. Even though in most models more than one field is involved, for simplicity in this section we will focus on the single-field scenario. The extension of this description to multiple-field models is straightforward. In the higher dimensional theory the scalar field parameterises the distance between the two boundary branes. A scalar field value of $-\infty$ corresponds to zero distance between the branes and thus represents the big crunch/big bang transition. There is an upper bound ϕ_{max} on the value of the scalar field, which implies that there is a finite maximum brane distance. In order to generate a cyclic universe, the potential $V(\phi)$ has to fulfil a number of constraints [69]:

- For $\phi > 0$ the potential needs to approach a shallow, positive plateau.

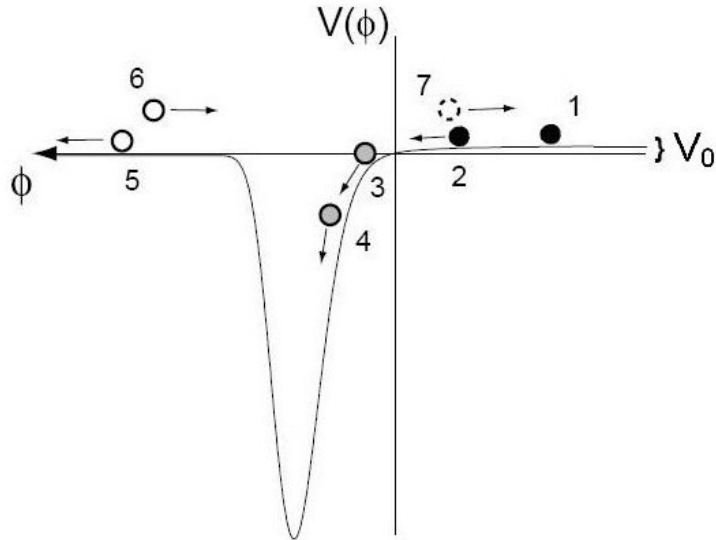


Figure 1: A possible shape of the interbrane potential $V(\phi)$ in the cyclic scenario. The behaviour of the scalar field ϕ with respect to this potential is shown. The plot has been reproduced from [29]. Black, grey, white and broken circles correspond to dark energy domination, the ekpyrotic phase, kinetic energy domination and radiation domination, respectively. Details about the different stages 1 - 7 can be found in the article.

- For $\phi_{end} < \phi < 0$ the potential needs to be negative and steeply decreasing as ϕ decreases. Here, ϕ_{end} is the scalar field value at the minimum of the potential $V_{,\phi}(\phi_{end}) = 0$.
- For $\phi \rightarrow -\infty$ the potential rapidly approaches zero $V(\phi) \rightarrow 0$.

It should be noted that there is some freedom in the first and third conditions, so that there are a number of different potentials that can lead to a cyclic universe. An example of a potential fulfilling these conditions and thus leading to a successful realization of the cyclic model is depicted in figure 1. Using this example of a cyclic potential the different stages of a cycle can be described.

One can start the cycle at the dark energy dominated universe today, with equation of state $w \approx -1$ (stage 1). At this stage the energy density of the universe is dominated by the potential energy of the scalar field and the expansion is slowly accelerating. The scalar field is either very close to or has already passed its maximum value. It then starts slowly rolling down the shallow plateau of the potential of positive height V_0 towards negative values

of ϕ (stage 2). For a scalar field ϕ with potential $V(\phi)$, when neglecting the matter and radiation contributions to the energy density and pressure, the second Friedmann equation (10) reads

$$\frac{\ddot{a}}{a} = -\frac{8\pi G}{3}(\dot{\phi}^2 - V(\phi)). \quad (109)$$

Therefore, accelerated expansion $\ddot{a} > 0$ is only given as long as $V(\phi) > \dot{\phi}^2$. The scalar field kinetic energy becomes important as $V(\phi)$ approaches zero. Acceleration stops, but the scale factor is still growing and the universe is in a state of decelerating expansion as the potential becomes negative (stage 3). At some point the kinetic energy exactly cancels the negative potential energy $\dot{\phi}^2/2 = -V(\phi)$ and according to the first Friedmann equation (15), again neglecting the radiation and matter components, the Hubble parameter is zero $H(t) = 0$. From (109) one can see that at this point $\ddot{a}(t) < 0$. Therefore, the universe reversed from expansion to slow contraction and the Hubble parameter becomes negative. The scalar field enters the ekpyrotic phase with $w \gg 1$ and is rolling down the steep, nearly exponential potential (stage 4). This period is of vital importance, since during it density fluctuations are created, which ultimately lead to the formation of large scale structure. As the scalar field rolls down the potential its kinetic energy grows. It moves past the potential minimum at ϕ_{end} and continues towards $\phi \rightarrow -\infty$. Potential energy is converted to scalar field kinetic energy and the evolution of the universe becomes increasingly kinetic energy dominated. The equation of state becomes $w \approx 1$. The scale factor $a(t)$ decreases and as the universe approaches the bounce the potential energy tends to zero $V(\phi) \rightarrow 0$ (stage 5). The scalar field takes a finite amount of time to reach negative infinity. The scale factor becomes zero at the big crunch/big bang, reverses and starts increasing again, the universe expands. It should be noted that while the four-dimensional scale factor $a(t)$ becomes zero at the big crunch, in the higher dimensional picture the brane scale factors remain finite at the collision. At the big crunch some of the kinetic energy of the scalar field is converted to relativistic and non-relativistic matter and the post-big bang universe is reheated to a large, finite temperature. After the big bang there is an expanding kinetic phase (stage 6), almost symmetrical to the contracting kinetic phase preceding the big bang, except that the scalar field acquires a small boost at the bounce. This is needed for the field to overcome Hubble damping due to radiation and increase enough to reach positive values again. In fact, after the big bang there are two kinetic energy dominated phases, separated by a very short $w \gg 1$ phase. However, it has been shown that all these phases can effectively be treated as just one kinetic phase [70]. While immediately after the bounce the universe is still kinetic energy dominated,

during the expanding phase this energy is rapidly redshifted away and the universe soon enters the radiation dominated epoch (stage 7). The scalar field experiences Hubble damping during radiation domination and the following matter dominated epoch, which correspond to $w = 1/3$ and $w = 0$, respectively. These two epochs are exactly the same as in the standard hot big bang picture. The structure that exists in these phases was seeded during the ekpyrotic phase preceding the big crunch/big bang transition. The field reaches its maximum value $\phi_{max} > 0$, turns around and starts slowly rolling down the potential plateau again. The potential energy of the scalar field comes to dominate over the radiation and matter components and the universe returns to the accelerating dark matter dominated stage (stage 1), where the cycle started.

A possible expression for a potential with the properties described above is

$$V(\phi) = V_0(e^{b\phi} - e^{-c\phi})F(\phi), \quad (110)$$

where $0 \leq b \ll 1$ and $c \gg 1$. $F(\phi)$ is a function that approaches unity for $\phi > \phi_{end}$, where ϕ_{end} is the scalar field value at the minimum of the potential $V(\phi)$, and rapidly becomes zero as ϕ drops below ϕ_{end} . As long as it satisfies these conditions the exact form of the function $F(\phi)$ is not important for the success of the cyclic model. The constant V_0 corresponds roughly to the value of the dark energy density observed today. It should be noted that during the ekpyrotic phase $\phi_{end} < \phi < 0$, so that the negative exponential in (110) dominates and the expression for the potential can be approximated by $V(\phi) \approx -V_0e^{-c\phi}$. This is the ekpyrotic potential that is known from (103) in the previous section.

During each cycle the universe undergoes a large net expansion. The approximate number of e-folds by which the scale factor grows per cycle is [70]

$$N_{de} + N_r + \frac{2\gamma_{ke}}{3}. \quad (111)$$

Here, N_{de} is the number of e-folds of dark energy domination, N_r is approximately the number of e-folds of matter and radiation domination and the last term quantifies the expansion during the kinetic energy dominated phase(s). During the ekpyrotic phase the scale factor decreases by a very small amount, so that its contribution to the overall change of the scale factor during a cycle can be neglected. In contrast to this large net expansion, some quantities undergo a periodic evolution and return to their original value after each cycle. This is true for example for the Hubble parameter. It is decreasing during the standard hot big bang evolution and during kinetic energy domination.

During the dark energy dominated epoch it is approximately constant. In the ekpyrotic phase it undergoes a large increase which balances the decrease in the preceding phases. This leads to the condition [70]

$$N_{ek} \approx 2(N_r + \gamma_{ke}), \quad (112)$$

where N_{ek} is defined by the growth of the Hubble parameter which increases by a factor of $e^{N_{ek}}$ during the ekpyrotic phase. (112) is the condition that needs to be fulfilled for the Hubble parameter to return to its original value after each cycle. Other locally measurable quantities also undergo zero net change per cycle, most notably the entropy density. Typical values for the number of e-folds of the respective regimes are for example $N_r \approx 55$, $\gamma_{ke} \approx 7$ and $N_{de} \approx 60$ [41, 31]. From (112) this leads to $N_{ek} \approx 124$. Also, from (111) it can be seen that for these values the scale factor grows by a factor of approximately e^{120} every cycle.

The evolution of the cyclic universe can be described by the first and second Friedmann equations, given in (1) and (10). The background metric is the flat, homogeneous and isotropic Friedmann-Robertson-Walker metric (12). The energy density of the universe is composed of a scalar field, radiation and non-relativistic matter. The radiation energy density ρ_r and the matter energy density ρ_m are both coupled to the scalar field. This coupling is given by a function $\beta(\phi)$. Using the expression for the energy density of a scalar field ρ_ϕ in (13), the first Friedmann equation (1) reads

$$H^2 = \frac{8\pi G}{3} \left(\frac{1}{2} \dot{\phi}^2 + V(\phi) + \beta^4(\phi)(\rho_r + \rho_m) \right). \quad (113)$$

Using the expressions for the energy density and pressure of a scalar field (13) and (14) and recalling that for radiation $p_r = \rho_r/3$, while for matter $p_m = 0$, the second Friedmann equation (10) is found to be

$$\frac{\ddot{a}}{a} = -\frac{8\pi G}{3} \left(\dot{\phi}^2 - V(\phi) + \beta^4(\phi) \left(\rho_r + \frac{1}{2} \rho_m \right) \right). \quad (114)$$

The coupling $\beta(\phi)$ is of crucial importance to the cyclic model. The matter and radiation energy densities couple to the effective scale factor of the brane $a\beta$ instead of the usual four-dimensional scale factor a , so that $\rho_r \propto (a\beta)^{-4}$ and $\rho_m \propto (a\beta)^{-3}$. By choosing β appropriately one can ensure that $a\beta$ becomes constant and nonzero as $a \rightarrow 0$ [36]. Therefore, due to their coupling to the scalar field ϕ , the energy densities of matter and radiation are finite at the big crunch. Using the energy conservation equation in (16), where ρ and p represent the sum of all energy densities and pressures that are present,

respectively, and making use of the scaling of the matter and radiation densities with the brane scale factor, the equation governing the evolution of the scalar field ϕ can be found. It is given by

$$\ddot{\phi} + 3H\dot{\phi} = -V_{,\phi} - \beta_{,\phi}\beta^3\rho_m. \quad (115)$$

It can be seen that the radiation density does not show up in this dynamical equation of motion. This makes sense, because for $\rho_r \propto (a\beta)^{-4}$ the term $\beta^4(\phi)\rho_r$ is independent of ϕ .

The ekpyrotic phase is preceded by a period of dark energy domination. During this period of accelerated expansion the radiation and matter densities become negligible, therefore the equations of motion describing ekpyrosis are dominated by the scalar field and its potential. When neglecting the radiation and matter components the first Friedmann equation (113) and the equation of motion for the scalar field (115) reduce to the single-field equations of motion (15) and (18) respectively. These are the same equations as found in section 4.1 when discussing the dynamics of the ekpyrotic phase. Since we also found that in the ekpyrotic period the cyclic potential (110) reduces to the ekpyrotic potential $V(\phi) \approx -V_0 e^{-c\phi}$, during the ekpyrotic phase of the cyclic model the scaling solution (104) can indeed be used. Similarly, a scaling solution for the kinetic energy dominated phase can be derived. During this phase the radiation and matter energy densities can again be neglected. Additionally, the potential tends to zero as ϕ decreases. Therefore, in this phase one can approximate $V(\phi) \approx 0$, $V_{,\phi}(\phi) \approx 0$. The first Friedmann equation in the cyclic model (113) then reduces to

$$H^2 = \frac{4\pi G}{3}\dot{\phi}^2. \quad (116)$$

The equation of motion for the scalar field (115) is also significantly simplified

$$\ddot{\phi} + 3H\dot{\phi} = 0. \quad (117)$$

Then, from (116) one can find that the scale factor depends on the scalar field as $a(\phi) \propto e^{\sqrt{\frac{4\pi G}{3}}\phi}$. Using this and the evolution equation for the scalar field (117) one can find an expression for $\phi(t)$ during kinetic energy domination which can then be used to find the dependence of the scale factor on time. This leads to the scaling solution in the kinetic energy dominated phase

$$a(t) \propto (-t)^{\frac{1}{3}}, \quad \phi(t) = \sqrt{\frac{1}{12\pi G}}\log(-t) + \phi_0, \quad (118)$$

where ϕ_0 is a constant. From this expression one can see that the kinetic energy density scales as a^{-6} . One should recall that the anisotropy energy density scales with the same power of a . This implies that the relative importance of anisotropies after the ekpyrotic phase is constant as the big crunch is approached.

An important variation of the cyclic model, the so-called *Phoenix Universe*, has recently been proposed [31, 32]. While the discussion above focussed on the single-field version of the cyclic model, this scenario unfortunately does not lead to the generation of scale-invariant curvature perturbations [27]. The most popular approach to generating the required spectrum of perturbations is the entropic mechanism [28]. The cyclic model of the universe that relies on this mechanism is called the phoenix universe. The entropic mechanism requires at least two scalar fields that evolve along an unstable classical trajectory during the ekpyrotic phase. This mechanism will be discussed in detail in section 4.4. Even though the correct scalar perturbation spectrum is generated, due to the instability of the trajectory a large part of the universe is diverted from it by quantum fluctuations, inhomogeneities grow and eventually almost the entire universe becomes trapped inside black holes. This leads to an important modification of the cyclic universe scenario discussed above. While in the single-field case virtually the entire universe survives after each cycle, in the phoenix universe an extremely large fraction of the universe does not make it through the ekpyrotic phase. The cyclic model is saved by the phase of accelerated expansion that precedes ekpyrosis. If this phase lasts sufficiently long, the region of space that can stay on the classical trajectory during ekpyrosis expands enough to, after the big bang, form the flat and homogeneous universe observed today. In the single-field model only a few e-folds of accelerated expansion were required to ensure that the cyclic model was a stable attractor. In contrast, in the phoenix universe a much longer duration of this phase is needed. The required number of e-folds is roughly [31]

$$N_{de} > N_{ek} - N_r - \frac{2\gamma}{3}. \quad (119)$$

Using the approximate values $N_r \approx 55$, $\gamma \approx 7$ [41] and the resulting $N_{ek} \approx 124$ which was found above gives $N_{de} > 64$. If this requirement is satisfied, a tiny initial patch that fulfils the right conditions will grow from cycle to cycle and lead to a sufficiently large homogeneous and isotropic domain to represent the observable universe. One can picture this evolution as most of the universe turning to "ash" at the end of each cycle, while only a tiny fraction makes it to the next cycle to form a new flat, homogeneous and isotropic universe. This explains the name "phoenix universe".

4.3 The Ekpyrotic/Cyclic Universe and the Cosmological Problems

Flatness problem

A phase of ekpyrotic contraction preceding the big bang can account for the flatness of the universe observed today. Using (21) it can be seen that in a contracting universe the energy density component with equation of state $w \gg 1$ dominates the evolution, while the relative importance of the spatial curvature rapidly decreases. Therefore, the universe becomes increasingly flat during the ekpyrotic phase.

To quantify this statement, one should recall the expression for the cosmological parameter $\Omega(t)$ given in (3). It is known from (104) that the scale factor is slowly decreasing during the ekpyrotic phase, while the Hubble parameter is growing rapidly. Therefore, during the ekpyrotic phase $a(t)$ can be approximated to be constant. The relation in (4) can then be written as

$$\frac{\Omega(t_e^{ek}) - 1}{\Omega(t_b^{ek}) - 1} \approx \left(\frac{H(t_b^{ek})}{H(t_e^{ek})} \right)^2 = e^{-2N_{ek}}, \quad (120)$$

where t_b^{ek} and t_e^{ek} are the times at which the ekpyrotic phase begins and ends, respectively. Since from (104) it is known that during ekpyrosis $H(t) \propto t^{-1}$, this can be rewritten in terms of t_b^{ek} and t_e^{ek} . (120) then reads

$$\frac{\Omega(t_e^{ek}) - 1}{\Omega(t_b^{ek}) - 1} \approx \left(\frac{t_e^{ek}}{t_b^{ek}} \right)^2. \quad (121)$$

Since the big crunch/big bang transition occurs at $t = 0$, $|t|$ is decreasing during the ekpyrotic phase. Therefore, the ratio in (121) is smaller than unity and the universe is flattened during the contraction.

Today the cosmological parameter is of order unity. The ekpyrotic phase is separated from a state of the universe as observed today by a period of acceleration during which the cosmological parameter will become even closer to unity. Therefore, one can use $\Omega(t_b^{ek}) - 1 \approx \mathcal{O}(1)$. Furthermore, let us assume that the radiation dominated phase starts at the Planck time. While this is certainly an overestimate, it will provide a good idea of how stringent the conditions on the duration of the ekpyrotic phase have to be to solve the flatness problem. At the Planck time the value of the cosmological parameter is $\Omega(t_{pl}) - 1 < 10^{-60}$, as known from section 2. Assuming that a flat

universe can re-emerge as such after the big crunch, and that the value of the cosmological parameter at the end of the ekpyrotic phase is approximately the same as at the beginning of radiation domination, one can find from (121) that

$$|t_b^{ek}| > 10^{30} |t_e^{ek}|. \quad (122)$$

If the ekpyrotic phase ends sufficiently close to the big crunch/big bang transition, this will lead to a short minimum duration. Assuming that the ekpyrotic phase ends approximately $10^3 t_{pl}$ before the big crunch, as suggested in [41], we find

$$|t_b^{ek}| > 10^{30} \cdot 10^3 \cdot 10^{-43} s = 10^{-10} s. \quad (123)$$

Compared to cosmological time scales this is a very short minimum duration, so that the condition for solving the flatness problem is easily fulfilled. This condition can be reformulated in terms of N_{ek} . Using the same approximations as above, from (120) it can be found that solving the flatness problem requires $N_{ek} \geq 70$. As was discovered in section 4.2, in the cyclic model a typical value is $N_{ek} \approx 120$. Therefore, the requirement on N_{ek} is easily fulfilled and the flatness problem can be solved.

Between the ekpyrotic phase and the onset of radiation domination there is a kinetic energy dominated phase. In order for the above considerations to be valid we have to make sure the flatness accomplished during the ekpyrotic phase is not destroyed during kinetic energy domination. The scale factor undergoes a net increase of a factor $e^{\frac{2\gamma_{ke}}{3}}$ in this phase. Using the scaling solution (118) this leads to a shrinking of the Hubble parameter $H(t) \propto a^{-3}(t)$ by a factor of $e^{-2\gamma_{ke}}$. Using (4) it can then be found that during the kinetic energy dominated phase the cosmological parameter changes as

$$\frac{\Omega(t_e^{kin}) - 1}{\Omega(t_b^{kin}) - 1} = e^{\frac{8\gamma_{ke}}{3}}, \quad (124)$$

where $t_b^{kin} \approx t_e^{ek}$ and t_e^{kin} are the times at which kinetic energy domination begins and ends, respectively. Since $\gamma_{ke} > 1$, during this phase the universe becomes less flat. For example, $\gamma_{ke} \approx 7$ [41] would lead to a ratio of approximately $e^{19} \approx 10^8$. Therefore, in order to solve the flatness problem, a longer duration of the ekpyrotic phase than given in (123) is needed. However, the effect of the kinetic energy dominated phase is relatively small and the resulting required duration is still very short, so that the flatness problem can easily be solved.

Homogeneity/Horizon problem

The universe that we observe today is incredibly homogeneous within the horizon. From (21) it can be seen that if a scalar field component with equation of state $w \gg 1$ is present in a slowly contracting universe, the relative importance of the anisotropy term decreases and the scalar field comes to dominate the energy density. Therefore, during the ekpyrotic phase the universe becomes increasingly homogeneous. During the following kinetic energy dominated phase with equation of state $w \approx 1$ the anisotropy term is constant relative to the scalar field energy density, so that the homogeneity generated during the ekpyrotic phase is preserved.

In the cyclic model the universe was not created at the big bang, but has been in existence for a large number of cycles, possibly infinitely many. It was shown in section 4.2 that the scale factor undergoes a large net increase every cycle. Therefore, in the previous cycle the region that is inside our horizon today was only a few kilometres in diameter. The Hubble parameter returns to its original value after each cycle, so that the Hubble radius $H^{-1}(t)$ today has a similar value as it had at this stage of the previous cycle. Therefore, even though earlier in the hot big bang phase the regions making up the observable universe were causally disconnected, they had plenty of time to be in causal contact in the previous cycle. This explains why the universe is so homogeneous on large scales within the horizon.

Origin of large-scale structure

During the ekpyrotic phase cosmological perturbations can be generated that lead to the formation of galaxies and temperature fluctuations in the microwave background after the big bang. Scalar density perturbations with a nearly scale-invariant spectrum can be formed, which then seed the formation of large-scale structure in the next cycle. The origin of these perturbations can be explained using the higher dimensional braneworld picture. The two boundary branes become very flat and parallel when approaching each other during the ekpyrotic phase. However, during the brane movement quantum fluctuations cause small ripples in the branes, leading to differences in the exact time of collision across the branes. Since areas where the collision takes place earlier have more time to cool, the result is small fluctuations in the temperature across the universe that can be observed in the cosmic microwave background.

In order to explain the origin of the modes that enter the horizon during the hot big bang phase, a similar strategy as in inflationary cosmology is applied. The modes were once in causal contact, but left the horizon during the ekpyrotic phase. To accomplish this they had to increase in size relative to the horizon. In the ekpyrotic phase this is achieved due to a rapidly decreasing Hubble radius $|H(t)|^{-1}$, so that the horizon is shrinking, while the size of the fluctuation modes stays approximately the same. Therefore, the quantum fluctuations eventually span superhorizon scales. Modes leave the horizon during the ekpyrotic phase and eventually re-enter it during the hot big bang phase. Due to gravity these perturbations then grow with time and ultimately lead to the formation of large structures.

During the ekpyrotic phase both scalar and tensor perturbations are generated. The ekpyrotic model also predicts the generation of a significant amount of non-gaussianity. The detailed calculations of the spectra of scalar and tensor perturbations will be given in section 4.4.

Monopole problem

The cyclic universe scenario manages to explain the absence of magnetic monopoles and other topological defects in a simple manner. In this model the matter in the universe is created at a slightly inelastic collision of branes. At this collision some of the scalar field kinetic energy is converted to radiation and non-relativistic matter and the hot big bang phase begins. The collision happens at a finite temperature, so that the temperature of the reheated universe is also finite. The mass scale at which unwanted relics are produced coincides with the mass scale of grand unified theories of approximately 10^{16} GeV. If the maximum temperature that is reached in the cyclic universe lies well below this scale, formation of heavy topological defects will be highly suppressed. This can explain why a negligible abundance of magnetic monopoles is observed.

4.4 Generation of Cosmological Perturbations

In the ekpyrotic/cyclic model of the universe density fluctuations are generated during the ekpyrotic phase preceding the big bang. These fluctuations seed the formation of large-scale structures during the hot big bang phase. In this scenario both scalar and tensor perturbations are generated. In the fol-

lowing first the scalar perturbations will be analysed to linear order, then the non-gaussian corrections will briefly be discussed and finally the spectrum of tensor perturbations will be calculated.

Scalar perturbations

The generation of scalar perturbations in the ekpyrotic/cyclic universe differs somehow from the mechanism applied in single-field inflation that was discussed in section 3.3. The fluctuations of only one scalar field cannot lead to the generation of a perturbation spectrum with the required properties during the ekpyrotic phase. For generation of the correct spectrum at least two fields have to be present. In the single-field case the Newtonian potential Φ does acquire a nearly scale-invariant spectrum, but the spectrum of the curvature perturbation on comoving hypersurfaces \mathcal{R} turns out to be very blue [27, 71, 72]. Such a spectrum is observationally excluded [3]. The explanation for this is that Newtonian potential and curvature perturbations correspond to two different modes that do not mix. In a contracting universe the Newtonian potential corresponds to a growing mode time-delay perturbation. The curvature perturbation, which is the growing mode in an expanding universe, corresponds to the decaying mode in the ekpyrotic phase. Therefore, in a single-field ekpyrotic model a scale-invariant spectrum of curvature perturbations cannot be obtained.

There are several ways to tackle this problem. One approach is to employ mixing of the Newtonian potential and the curvature perturbation at the bounce. When the two types of modes mix the time-delay mode could dominate on large scales, leading to a nearly scale-invariant perturbation spectrum after the big bang. Such models usually employ higher dimensional effects and the breakdown of the four-dimensional effective theory close to the big crunch. Examples for such a mixing have for example been given in [73, 74]. Unfortunately, a complete five-dimensional description of the scenario does not exist and matching the description at the bounce with the effective four-dimensional theory remains difficult.

A different approach in which an almost scale-invariant spectrum of curvature perturbations can be obtained before the big bang has recently been discovered, the entropic mechanism [28, 75]. A major advantage of this approach is that it can fully be described by ordinary four-dimensional effective physics. In the following we will rely on this mechanism in order to demonstrate how a nearly flat spectrum of curvature perturbations can be generated

in the ekpyrotic/cyclic model. The entropic mechanism requires the presence of at least two scalar fields, which move along an unstable classical trajectory. In the higher dimensional set-up underlying the model, the presence of two scalar fields can easily be accommodated [65, 66]. One of the fields parameterises the separation of the two boundary branes, while the other one corresponds to the volume modulus of the internal Calabi-Yau manifold. During the ekpyrotic phase both fields roll down a steep, negative potential, so that each field develops nearly scale-invariant perturbations. This leads to a nearly scale-invariant spectrum of entropy perturbations, which in a collapsing universe corresponds to a growing mode [76]. This spectrum can be converted to a spectrum of curvature perturbations with the same properties before the big crunch. Such a conversion can for example be achieved using a bounce of the four dimensional scalar field trajectory at a boundary in moduli space when approaching the big crunch/big bang transition. Such boundaries do occur naturally in the higher dimensional theory, as will be discussed below. After the big bang the entropy perturbations decay and only the nearly scale-invariant spectrum of curvature perturbations, which are growing mode perturbations in an expanding universe, is left to seed the large-scale structures observed today.

The following analysis of the entropic mechanism of generating scalar perturbations during the ekpyrotic period is based on the calculation in [28]. Part of the calculation is very similar to the corresponding derivation in single-field inflation, so that for the details of these steps the reader will be referred to section 3.3.

The action describing the generation of entropy perturbations via the entropic mechanism is the two-field version of the ekpyrotic action (100)

$$S = \int d^4x \sqrt{-g} \left(-\frac{R}{16\pi G} + \frac{1}{2} \partial_\mu \phi_1 \partial^\mu \phi_1 + \frac{1}{2} \partial_\mu \phi_2 \partial^\mu \phi_2 - V(\phi_1, \phi_2) \right). \quad (125)$$

This is the action for two scalar fields with canonical kinetic energy that interact only through gravity. The background evolution is described by the two-field version of the scaling solution given in (104). Both of the fields roll down a steep, negative potential. The overall potential $V(\phi_1, \phi_2)$ is therefore given by the sum of two ekpyrotic potentials

$$V(\phi_1, \phi_2) = -V_1 e^{-\int c_1 d\phi_1} - V_2 e^{-\int c_2 d\phi_2}, \quad (126)$$

where c_i is a slowly varying function of the corresponding scalar field $c_i = c_i(\phi_i)$ and $V_1, V_2 > 0$ are positive constants. In the following it will be assumed that the two fields simultaneously approach $-\infty$. The dynamics of

this system can be described in terms of two new variables σ and s [77, 78]. σ defines the ekpyrotic or adiabatic direction pointing along the trajectory. s defines the direction transverse to the trajectory and thus transverse to σ . The two variables are given by a rotation in field space

$$\sigma = \cos \theta \phi_1 + \sin \theta \phi_2, \quad s = \cos \theta \phi_2 - \sin \theta \phi_1, \quad (127)$$

where θ is the angle of the field space trajectory. In the following calculations it will be useful to work with the time-derivative of σ which is given by

$$\dot{\sigma} = \sqrt{\dot{\phi}_1^2 + \dot{\phi}_2^2}. \quad (128)$$

The equation of motion for σ can be found by adding up the equations governing the evolution of the two scalar fields ϕ_1, ϕ_2 given in (102) and making use of the expression for $\dot{\sigma}$ (128). It is found to be

$$\ddot{\sigma} + 3H\dot{\sigma} + V_{,\sigma} = 0, \quad (129)$$

with $V_{,\sigma} = V_{,\phi_1} \cos \theta + V_{,\phi_2} \sin \theta$. This expression for $V_{,\sigma}$ could alternatively be written entirely in terms of the two scalar fields and the potential by using that [79]

$$\cos \theta = \frac{\dot{\phi}_1}{\dot{\sigma}}, \quad \sin \theta = \frac{\dot{\phi}_2}{\dot{\sigma}}. \quad (130)$$

One can take the derivative of one of these expressions and use the evolution equations for the scalar fields and σ given in (102) and (129), respectively. After substituting the expressions involving θ using (130) one can find an equation relating the change of the angle of the background trajectory in time to the potential defined in (126)

$$\dot{\theta} = \frac{V_{,\phi_1} \dot{\phi}_2 - V_{,\phi_2} \dot{\phi}_1}{\dot{\sigma}^2}. \quad (131)$$

Now that the general scenario is set up the behaviour of the perturbations can be analysed. Using the variables σ and s one can identify two different types of perturbations. Entropy or isocurvature perturbations δs are perturbations transverse to the direction of the background trajectory, i.e. along the entropic direction defined by s . Perturbations along the ekpyrotic direction σ and thus along the trajectory correspond to adiabatic or curvature perturbations $\delta\sigma$. From (127) the perturbations can be found and, after substituting (130), are given by

$$\delta\sigma = \frac{\delta\phi_1 \dot{\phi}_1 + \delta\phi_2 \dot{\phi}_2}{\dot{\sigma}}, \quad \delta s = \frac{\delta\phi_2 \dot{\phi}_1 - \delta\phi_1 \dot{\phi}_2}{\dot{\sigma}}. \quad (132)$$

Both of these perturbation modes are gauge-invariant. Here, the variable of interest is the entropy perturbation δs , since in a contracting universe δs corresponds to a growing mode.

It should be noted that due to the presence of more than one scalar field the background trajectory is unstable to small perturbations [28, 80]. In fact, it moves along a ridge of the potential [77] and has to follow it closely for a sufficient amount of time for this model to work. This is precisely what led to the modification of the cyclic universe scenario that was discussed at the end of section 4.2, the so-called phoenix universe.

The general equation of motion for the entropy perturbation in Fourier space is found for example in [79] and reads

$$\ddot{\delta s} + 3H\dot{\delta s} + \left(3\dot{\theta}^2 + \frac{k^2}{a^2} + V_{,ss}\right) \delta s = \frac{1}{2\pi G} \frac{\dot{\theta}}{\dot{\sigma}} \left(\frac{k}{a}\right)^2 \Phi. \quad (133)$$

Here, $V_{,ss}$ is the second derivative of the potential $V(\phi_1, \phi_2)$ with respect to the variable s . To simplify the analysis of this equation it will be assumed that the trajectory is given by a straight line in field space, such that the angle of the trajectory does not change in time $\dot{\theta} = 0$. In fact, from the scaling solutions in (104) and (118) one can see that $\dot{\phi}_i \propto t^{-1}$. This implies that $\tan(\theta) = \dot{\phi}_1/\dot{\phi}_2$ is time independent, and thus taking $\dot{\theta} = 0$ is a well-motivated approximation during the ekpyrotic and kinetic phases. As can be seen from (130) this also implies that the time derivatives of the two scalar fields are the same up to a constant factor $\dot{\phi}_1 = \dot{\phi}_2/\gamma$, with γ a constant which is usually of order unity. Additionally, from (131) one can see that this approximation leads to a constraint on the potential, given by

$$V_{,\phi_1}\dot{\phi}_2 - V_{,\phi_2}\dot{\phi}_1 = 0. \quad (134)$$

Using the proportionality of $\dot{\phi}_1$ and $\dot{\phi}_2$ one can integrate this to find

$$V(\phi_1, \phi_2) = V'(\phi_1) + \gamma^2 V' \left(\frac{\phi_2}{\gamma} \right), \quad (135)$$

where V' is some function and a constant term has been ignored.

For a straight trajectory the source term on the right hand side of the equation of motion for the entropy perturbation (133) vanishes and the equation simplifies to

$$\ddot{\delta s} + 3H\dot{\delta s} + \left(\frac{k^2}{a^2} + V_{,ss}\right) \delta s = 0. \quad (136)$$

We would like to have an equation of motion of the same form as (69), so that the results of section 3.3 can be used. To achieve this a new variable $v = a\delta s$ is introduced and substituted for the density perturbation. Also, from now on conformal time τ instead of cosmological time t will be used. The equation of motion in (136) then reads

$$v_{,\tau\tau} + \left(k^2 - \frac{a_{,\tau\tau}}{a} + a^2 V_{,ss} \right) v = 0. \quad (137)$$

In order to solve this equation the term in the brackets preceding v will be expressed in terms of the fast-roll parameter $\bar{\epsilon}$, which has been defined in (106), and its derivative with respect to $M \equiv \ln(a(t)/a(t_{end}^{ek}))$. In the following, derivatives of $\bar{\epsilon}$ with respect to M of second order, $\bar{\epsilon}_{,MM}$, and higher will be neglected and the results will be given to sub-leading order in $\bar{\epsilon}$.

The first expression of interest in (137) is $a_{,\tau\tau}/a$. This can be rewritten in terms of the fast-roll parameter by using its definition in (106), substituting \dot{H} by the scale factor and its derivatives and rewriting the resulting expression in terms of conformal time. One finds that

$$\frac{a_{,\tau\tau}}{a} = \mathcal{H}^2(2 - \bar{\epsilon}). \quad (138)$$

The second term of interest is $a^2 V_{,ss}$. To express this in terms of the fast-roll parameter one should notice that the approximations used here imply that $V_{,\sigma\sigma} = V_{,ss}$. From the two-field versions of the equations of motion in the ekpyrotic phase, given in (101) and (102), one can see that $\dot{H} = -4\pi G(\dot{\phi}_1^2 + \dot{\phi}_2^2)$. One can then relate the fast-roll parameter $\bar{\epsilon}$ to the variable σ as

$$\bar{\epsilon} = 4\pi G \frac{\dot{\sigma}^2}{H^2}. \quad (139)$$

To find an expression for $V_{,ss} = V_{,\sigma\sigma}$ one should differentiate this expression twice with respect to time and use the fact that $\bar{\epsilon}_{,M} = H^{-1}\dot{\bar{\epsilon}}$ and that terms of order $\bar{\epsilon}_{,MM}$ are neglected. One should then differentiate the equation of motion for σ given in (129) and substitute derivatives of σ by expressions involving the fast-roll parameter. After a few calculations one obtains

$$V_{,ss} \approx H^2(6\bar{\epsilon} - 2\bar{\epsilon}^2 + \frac{5}{2}\bar{\epsilon}_{,M}). \quad (140)$$

The next step is to find an expression for \mathcal{H} in terms of conformal time. Such an expression can be derived using (138), which can be rewritten as

$$\frac{\mathcal{H}_{,\tau}}{\mathcal{H}^2} = 1 - \bar{\epsilon}. \quad (141)$$

This can be integrated to give

$$\frac{1}{\mathcal{H}} = \int_0^\tau d\tau \bar{\epsilon}(\tau) - \tau. \quad (142)$$

One can solve the remaining integral using a step-by-step procedure. The expression $1 = d(\tau)/d\tau$ is inserted under the integral and an integration by parts is carried out. After applying this procedure twice (142) reads

$$\frac{1}{\mathcal{H}} = -\tau + \tau \bar{\epsilon} - \tau^2 \bar{\epsilon}_{,\tau} + \int_0^\tau d\tau (\tau(\tau \bar{\epsilon}_{,\tau})_{,\tau}). \quad (143)$$

The remaining integral in this expression can be neglected. One can see this by rewriting the expression underneath the integral using $\bar{\epsilon}_{,\tau} = \mathcal{H} \bar{\epsilon}_{,M}$ and inserting an approximate expression for \mathcal{H} . Such an expression can be found by calculating the dependence of $a(t)$ in (104) on conformal time

$$a(\tau) \propto (-\tau)^{\frac{p}{1-p}}. \quad (144)$$

Assuming p is constant one can then write $\mathcal{H} = a_{,\tau}/a$ in terms of $\bar{\epsilon}$ and find that to leading order $\mathcal{H} \approx (\bar{\epsilon}\tau)^{-1}$. Using this one obtains

$$(\tau \bar{\epsilon}_{,\tau})_{,\tau} \tau \approx \left(\frac{\bar{\epsilon}_{,M}}{\bar{\epsilon}}\right)_{,\tau} \tau \approx \frac{1}{\bar{\epsilon}} \left(\frac{\bar{\epsilon}_{,M}}{\bar{\epsilon}}\right)_{,M}. \quad (145)$$

One can thus see that the integral in (143) is of $\mathcal{O}(\bar{\epsilon}^{-2})$, so that it can be neglected. An expression for \mathcal{H} can then be obtained from (143). It is given by

$$\mathcal{H} \approx \frac{1}{\tau} \frac{1}{(\bar{\epsilon} - 1 - \frac{\bar{\epsilon}_{,M}}{\bar{\epsilon}})}. \quad (146)$$

Again neglecting terms of $\mathcal{O}(\bar{\epsilon}^{-2})$ or higher one can find

$$\mathcal{H}^2 \approx \frac{1}{(\tau \bar{\epsilon})^2} \left(1 + \frac{2}{\bar{\epsilon}} + \frac{2\bar{\epsilon}_{,M}}{\bar{\epsilon}^2}\right). \quad (147)$$

Using this in combination with (138) and (140) the equation of motion for v in (137) reads

$$v_{,\tau\tau} + \left(k^2 - \frac{\nu_s^2 - \frac{1}{4}}{\tau^2}\right) = 0, \quad (148)$$

where

$$\nu_s^2 \approx \frac{3}{2} - \frac{1}{\bar{\epsilon}} + \frac{1}{2} \frac{\bar{\epsilon}_{,M}}{\bar{\epsilon}^2}. \quad (149)$$

This is exactly the same equation as (69), which was found during the analysis of the evolution of scalar perturbations during inflation, with $\nu_{\mathcal{R}}$ substituted

by ν_s and ν_k exchanged with ν . We are primarily interested in determining the spectral index n_s , since this will be contrasted with the value generated during inflation and compared to observations in section 5.2. The precise shape of the power spectrum is of less interest, because for an exact estimate of the amplitude of the curvature perturbations more details about the conversion process from entropy to curvature perturbations would have to be known. Following the same steps as in section 3.3 one can find the wavenumber-dependence of the variable v in the large-scale limit

$$|v(k)| \propto \frac{k^{\frac{1}{2}-\nu_s}}{\sqrt{k}}. \quad (150)$$

The power spectrum of the entropy perturbation $P_{\delta s}$ is defined as

$$P_{\delta s}(k) = \frac{k^3}{2\pi^2} |\delta s|^2. \quad (151)$$

Recalling that $\delta s = v/a$ and inserting this and (150) into (151) it can easily be seen that $P_{\delta s}(k) \propto k^{3-2\nu_s}$. The spectral index of the spectrum of entropy perturbations generated during the ekpyrotic phase is then given by

$$n_{\delta s} - 1 \equiv \frac{d \ln P_{\delta s}}{d \ln k} \approx \frac{2}{\bar{\epsilon}} - \frac{\bar{\epsilon}_{,M}}{\bar{\epsilon}^2}. \quad (152)$$

The positive term on the right-hand side is a gravitational contribution which tends to shift the spectrum to the blue. The negative term has a non-gravitational origin and shifts the spectrum to the red. Depending on which term dominates the ekpyrotic scenario can lead to a slightly blue or a slightly red spectrum. The fast-roll parameter is very large, usually of $\mathcal{O}(100)$, so that, independent of which one of the terms dominates, the deviation from scale-invariance is very small.

It has been shown that during a slowly contracting phase a nearly scale-invariant spectrum of entropy perturbations can be obtained using the entropic mechanism. However, what is observed today is a spectrum of nearly scale-invariant curvature perturbations. Therefore, a mechanism to convert entropy perturbations to curvature perturbations is needed. Such a conversion can happen due to a bending of the trajectory in field space. There are different possibilities for how this type of conversion can take place. The most important conversion mechanisms are kinetic conversion [28], ekpyrotic conversion [77, 78] and conversion via modulated preheating [81].

For conversion via modulated preheating the conversion takes place shortly after the big bang. It relies on the presence of massive matter fields and their

coupling to ordinary matter, with a coupling strength that depends on the entropy perturbation δs . While this leads to a viable theory of conversion, its predictive power is limited, since the exact dependence of the coupling on δs is unknown.

The ekpyrotic conversion mechanism relies on the conversion taking place during the ekpyrotic phase, when the trajectory moves away from the ridge of the potential and falls off one of the sides. While this is an acceptable conversion mechanism, the resulting predictions for non-gaussianity [82] do not agree well with observations [19].

Due to the shortcomings of ekpyrotic conversion and conversion via modulated preheating, this review will focus on kinetic conversion. Curvature perturbations are created from entropy perturbations shortly before the big crunch, when the universe is in the kinetic energy dominated phase. This leads to predictions for the spectral tilt and non-gaussianity [82] that agree well with observations [19]. It should however be noted that, in order for the conversion not to happen during the ekpyrotic phase, the trajectory must stay very close to the ridge of the potential for a sufficiently long period of time.

Kinetic energy domination starts at the end of the ekpyrotic phase at time t_{end}^{ek} . For kinetic conversion of entropy perturbations to curvature perturbations a bending of the trajectory in scalar field space after this time is required. Such a bending occurs naturally in the higher-dimensional picture. As discussed at the beginning of section 4, the cyclic model can be described by a scenario in heterotic M-theory relying on the collision of two branes which have opposite tensions. The negative tension brane encounters a spacetime singularity shortly before the collision, at which the six-dimensional manifold shrinks to zero size [83]. In the effective four-dimensional theory this leads to a boundary between field and manifold space at $\phi_2 = 0$, so that the scalar field space is restricted to the half plane $-\infty < \phi_1 < +\infty, -\infty < \phi_2 < 0$. Close to the boundary at $\phi_2 = 0$ an effective repulsive potential becomes important. Due to this potential the background trajectory bounces off the boundary, leading to a bending of the trajectory just before the big crunch/big bang transition. This bounce is assumed to be elastic, so that none of the field's energy is lost.

This scenario illustrates that a bending of the trajectory taking place just before the big crunch can easily be accommodated in the higher-dimensional picture. To keep this discussion general, the following calculation will apply to any such bending occurring during kinetic energy domination, independent

of its origin.

The quantity of interest is the curvature perturbation on comoving hypersurfaces \mathcal{R} . The time derivative of this quantity can be found from the perturbed Einstein field equations and is given by [79]

$$\dot{\mathcal{R}} = \frac{H}{\dot{H}} \left(\frac{k^2}{a^2} \Psi - 8\pi G g_{ij} \frac{D^2 \phi^i}{Dt^2} s^j \right). \quad (153)$$

Here, Ψ is the potential defined in (38), $g_{ij}(\phi)$ is the Kähler metric and D^2/Dt^2 is the geodesic operator on scalar field space. Since the case of two scalar fields is considered, in this section Roman indices correspond to $i, j = 1, 2$. The quantity s^i is defined as

$$s^i = \delta\phi^i - \dot{\phi}^i \frac{g_{jk} \dot{\phi}^j \delta\phi^k}{g_{rs} \dot{\phi}^r \dot{\phi}^s}. \quad (154)$$

Since the analysis is carried out in flat scalar field space, the metric reduces to $g_{ij} = \delta_{ij}$. Also, the geodesic operator simplifies to a normal time derivative. The two variables s^1 and s^2 can then be calculated. Using the definition of the entropy perturbation δs in (132) one finds

$$s^1 = -\dot{\phi}_2 \frac{\delta s}{\dot{\sigma}}, \quad s^2 = \dot{\phi}_1 \frac{\delta s}{\dot{\sigma}}. \quad (155)$$

Combining this with (153) it can be seen that $\dot{\mathcal{R}}$ depends on the entropy perturbation δs , such that a nonzero entropy perturbation can source a curvature perturbation. One should note that our main interest is superhorizon entropy perturbations. Therefore, it is sufficient to work in the large-scale limit, in which the first term on the right-hand side of (153) can be neglected. This gives

$$\dot{\mathcal{R}} \approx -8\pi G \frac{H}{\dot{H}} \delta_{ij} \frac{D^2 \phi^i}{Dt^2} s^j. \quad (156)$$

It can be seen that for a straight line background trajectory in scalar field space one finds $\dot{\mathcal{R}} = 0$ and the entropy perturbation does not source the curvature perturbation. For a successful conversion a deviation from a straight trajectory is needed. We will assume that this deviation results from an instantaneous reflection of ϕ_2 off a boundary at $\phi_2 = 0$ at time t_b . It should be noted that, while this is a convenient choice, the results are actually independent of the exact position of the boundary or which of the two fields is reflected. The trajectory in field space can be described by

$$\dot{\phi}_2 \Big|_{t < t_b} = -\alpha \dot{\phi}_1, \quad \dot{\phi}_2 \Big|_{t > t_b} = +\alpha \dot{\phi}_1, \quad (157)$$

where $\alpha > 0$ is a constant and $\dot{\phi}_1$ is constant and negative $\dot{\phi}_1 < 0$ close to the bounce. This implies that before the bounce ϕ_2 was growing, while after the bounce it is decreasing. Since the bounce happens instantaneously it can be described by a delta function, so that

$$\frac{D^2\phi_2}{Dt^2} = 2\dot{\phi}_2(t_b^+)\delta(t - t_b). \quad (158)$$

Inserting this into (156) it can be seen that on large scales a nearly scale-invariant spectrum of entropy perturbations is instantaneously converted into a spectrum of curvature perturbations with the same properties.

In order to find an expression for the curvature perturbation on comoving hypersurfaces (156) needs to be integrated. Since conversion happens during the kinetic energy dominated phase, the calculation can be simplified by making use of the scaling relation (118). This relation implies that $H(t) = (3t)^{-1}$. Using this, inserting (158) and the expression for s^2 given in (155) into (156) and then evaluating the integral using the delta function, one finds

$$\mathcal{R} = 16\pi G \frac{\dot{\phi}_1 \dot{\phi}_2}{\sqrt{\dot{\phi}_1^2 + \dot{\phi}_2^2}} t_b \cdot \delta s(t_b). \quad (159)$$

Ultimately, the quantity of interest is the variance of the spatial curvature perturbation, $\langle \mathcal{R}^2 \rangle$. Making use of (157) and applying the two-field version of the first Friedmann equation (116) to substitute $\dot{\phi}_i$, one obtains

$$\langle \mathcal{R}^2 \rangle = \frac{64\pi G}{3} \frac{\alpha^2}{(1 + \alpha^2)^2} \langle \delta s^2 \rangle. \quad (160)$$

It can be seen that, in this approximation, the behaviour of the entropy perturbation gets directly translated into the curvature perturbation. Therefore, the spectrum of curvature perturbations inherits the spectral index and thus also the near scale-invariance from the entropy perturbation spectrum.

One can use the almost perfect scale-invariance of the entropy spectrum to get a rough idea of the value of $\langle \mathcal{R}^2 \rangle$. This is done by approximating $\langle \delta s^2 \rangle$ to be completely scale invariant, so that, after restoring the Planck constant \hbar , it is given by [28]

$$\langle \delta s^2 \rangle = \hbar \int \frac{dk}{4\pi^2} \frac{1}{kt^2}. \quad (161)$$

Unfortunately, this approximation is only valid until the end of the ekpyrotic phase at t_{end}^{ek} . At this time kinetic energy domination begins and the potential

becomes irrelevant. After inserting $H(t) = (3t)^{-1}$ the equation of motion (136) in the large scale approximation during kinetic energy domination reads

$$\ddot{\delta s} + \frac{\dot{\delta s}}{t} = 0. \quad (162)$$

This results in a logarithmic time-dependence of the entropy perturbation during the kinetic phase $\delta s = A + B \ln(-t)$. One should recall that during the ekpyrotic phase $\delta s \propto t^{-1}$. By requiring the expressions for δs during the kinetic phase and the ekpyrotic phase and the corresponding first derivatives to coincide at $t = t_{end}^{ek}$ one can determine the constants A and B . It is then found that during the kinetic energy dominated phase $\delta s(-t) = \delta s(-t_{end}^{ek})(1 + \ln(-t_{end}^{ek}) - \ln(-t))$. After inserting this and (161) and using that the time at which the ekpyrotic phase ends can be approximated as $t_{end}^{ek}{}^2 = 2(c^2|V(t_{end}^{ek})|)^{-1}$, (160) finally reads

$$\langle \mathcal{R}^2 \rangle = \hbar \frac{8\pi G}{3\pi^2} c^2 |V(t_{end}^{ek})| \left(\frac{\alpha^2}{(1 + \alpha^2)^2} \right) \left(1 + \ln \left(\frac{t_{end}^{ek}}{t_b} \right) \right)^2 \int \frac{dk}{k}. \quad (163)$$

This is of course just a rough estimate. However, it has been found that values of c and $V(t_{end}^{ek})$ that lead to a value of $\langle \mathcal{R}^2 \rangle$ that matches observations can easily be accommodated by heterotic M-theory [84]. Therefore, the cyclic model is able to achieve a realistic value for the amplitude of the curvature perturbations, which is an important finding for the consistency of the model.

One should note that in order for the ekpyrotic/cyclic model to have predictive power one has to make an assumption about how the pre-big bang contracting universe passes through the singularity and matches onto the post-big bang expanding universe. There are many different theories about the dynamics at the big crunch/big bang transition and their effect on the evolution of the spectrum of curvature perturbations (see e.g. [74, 72, 85, 63, 27, 86, 87, 71, 88, 89, 90, 60]). Unfortunately, no complete description of these dynamics has been developed so far. Therefore, in this paper it will be assumed that the exact dynamics at the bounce are not important, so that the generated perturbations can pass through the bounce unmodified [27]. Furthermore, it is assumed that the evolution of the perturbations is essentially unaffected by the dynamics in the early pre-big bang universe, up to the stage of nucleosynthesis. Of course, these assumptions need to be re-investigated as soon as the physics of the bounce is better understood.

Non-gaussianity

In the previous section the curvature perturbations generated via the entropic mechanism have been analysed to linear order. When extending this analysis to include higher-order terms one can find non-gaussian corrections to the calculated spectrum. A detailed calculation of the amount of non-gaussianity generated in the ekpyrotic/cyclic model is beyond the scope of this paper. For such a calculation see e.g. [82, 91]. However, since a strong non-gaussian signature is an important prediction of the model, in this section the results of these papers will be stated and a rough outline of the main steps of the calculation will be given.

Density perturbations are generated during the ekpyrotic phase when the scalar fields are rolling down a steep potential. Due to the steepness of the potential substantial non-linear self-interactions of the scalar fields are taking place during this process, leading to the generation of a large amount of non-gaussianity. The non-gaussianity predicted by the ekpyrotic/cyclic model is generally of local form [92]. In order to calculate the non-gaussian signature generated during the ekpyrotic phase, the calculation of the evolution of scalar perturbations given in the previous section has to be extended to include second-order terms. The analysis can also be carried out to higher orders in perturbation theory, however, the second order non-gaussianity is the most important contribution and we will limit our discussion to this. The entropy perturbation can then be written as $\delta s = \delta s^{(1)} + \delta s^{(2)}$, where $\delta s^{(1)}$ is the linear, gaussian part that has been analysed above and $\delta s^{(2)}$ corresponds to a second-order perturbation. The starting point for the calculation is the equation of motion in (136), extended to include second-order terms. Again the analysis can be carried out in the large-scale limit. By expanding the potential given in (126) up to third order in terms of σ and s and using the resulting expression to simplify the equation of motion, the entropy perturbation $\delta s(t)$ up to second order in the field perturbations can be found.

After the non-gaussianity in the entropy perturbation is generated it is imprinted on the curvature perturbation \mathcal{R} . Different possible conversion mechanisms have been discussed in the previous section. We will again assume that the conversion happens shortly before the big bang during kinetic energy domination. This is a valid choice, since the amount of non-gaussianity predicted by models that rely on conversion during the ekpyrotic phase [82] does not agree well with current data [19]. The resulting non-gaussian contribution to the curvature perturbation is the non-gaussianity that can be measured today. The evolution of the curvature perturbation on large scales

given in (156) also has to be extended to include second-order terms. The curvature perturbation on comoving hypersurfaces is then given by (77). As in the inflationary scenario, \mathcal{R}_0 is the gaussian curvature perturbation that has been calculated in the previous section and the second term corresponds to a non-gaussian contribution. The non-gaussianity parameter f_{NL} is the quantity that we wish to calculate. The contributions to this parameter can be subdivided into three parts $f_{NL} = f_{NL}^{intrinsic} + f_{NL}^{integrated} + f_{NL}^{reflection}$. The first parameter, $f_{NL}^{intrinsic}$, is a result of the nonlinearity in the entropy perturbation that is directly translated into non-linearity in the curvature perturbation. Therefore, this contribution is caused directly by self-interactions of the scalar fields during the ekpyrotic phase. The second term, $f_{NL}^{integrated}$, results from the nonlinear relation of the curvature perturbation and the entropy perturbation and is generated during the ekpyrotic phase. The last term, $f_{NL}^{reflection}$, has the same origin, but is generated during the process of conversion. The conversion takes place during the kinetic energy dominated epoch, therefore the equation of motion (162) applies in the large-scale limit. Assuming that the conversion is gradual, such that the second and higher time derivatives of the bending angle are zero, the evolution of the first and second order entropy perturbations during conversion can be studied.

After a few calculations the three contributions to f_{NL} can be found. The intrinsic contribution is found to be proportional to $\sqrt{\bar{\epsilon}}$, where $\bar{\epsilon}$ is the fast-roll parameter during the ekpyrotic phase defined in (106). The intrinsic contribution can be of either sign. $f_{NL}^{integrated}$ is independent of $\bar{\epsilon}$, so that it only shifts the overall result by a constant. The same is true for the reflected contribution, which corresponds to a negative shift. The exact value of the shift resulting from $f_{NL}^{reflected}$ and $f_{NL}^{integrated}$ depends on the properties of the conversion. The overall value of f_{NL} for conversion during the kinetic energy dominated phase is approximately given by [82]

$$f_{NL} \approx \frac{3}{2}c_3\sqrt{\bar{\epsilon}} + 5, \quad (164)$$

where c_3 is a constant of order unity. It can be seen that, depending on the sign of c_3 , the non-gaussianity parameter f_{NL} can be either positive or negative. For typical values of $\bar{\epsilon} \approx \mathcal{O}(100)$ f_{NL} is of order a few tens, which corresponds to a significant and soon detectable observational imprint. Also, due to the dependence on $\bar{\epsilon}$, there exists a correlation between the non-gaussianity and the spectral tilt. As can be seen from (152) the higher $\bar{\epsilon}$, the redder the spectral index n_{δ_s} . Using (164) this implies that the redder the spectral index, the larger the degree of non-gaussianity.

Tensor perturbations

During the ekpyrotic phase in addition to scalar perturbations a spectrum of primordial gravitational waves is generated. The analysis of tensor perturbations in the ekpyrotic/cyclic model is very similar to that in single-field inflation, therefore we refer to section 3.3 for further details of some steps in the calculation.

The perturbed background metric for the analysis of tensor perturbations was given in (79), where h_{ij} are the gauge-invariant tensor perturbations that are of interest here. The aim of this calculation is to determine the wavenumber-dependence of the tensor power spectrum $P_T(k)$, so that the corresponding spectral index n_T can be found. The first steps of the analysis are identical to the calculations in section 3.3. Therefore, the equation of motion that has to be solved is given by (86) and reads

$$f_{k,\tau\tau} + \left(k^2 - \frac{a_{,\tau\tau}}{a}\right) f_k = 0, \quad (165)$$

where the variable $f_k \equiv v_k$ has been defined to be able to distinguish between the calculations in this section and the calculations in section 3.3. To solve this equation an expression for $a_{,\tau\tau}/a$ valid during the ekpyrotic phase has to be found. Using the scaling of the scale factor with conformal time given in (144) one can find that

$$\frac{a_{,\tau\tau}}{a} = \frac{1}{\tau^2} \left(\frac{p^2}{(1-p)^2} - \frac{p}{1-p} \right). \quad (166)$$

Then, (165) can be written as

$$f_{k,\tau\tau} + \left(k^2 - \frac{\nu_T^2 - \frac{1}{4}}{\tau^2}\right) f_k = 0, \quad (167)$$

where the parameter ν_T depends on p and thus also on the fast-roll parameter $\bar{\epsilon} = 1/p$ as

$$\nu_T = \frac{1}{2} \left| \frac{1-3p}{1-p} \right| = \frac{1}{2} \left| \frac{\bar{\epsilon}-3}{\bar{\epsilon}-1} \right|. \quad (168)$$

This is exactly the same equation as given in (91), so that the same solution mechanism as in section 3.3 can be applied. Using (92) and (93) and recalling that $f_k = v_k$ the tensor power spectrum P_T is given by

$$P_T(k) = 64\pi G \frac{k^3}{2\pi^2} \frac{|f_k|^2}{a^2}. \quad (169)$$

Using the wavenumber-dependence of $f_k = v_k$ in the large-scale limit given in (73) and replacing $\nu_{\mathcal{R}}$ with ν_T , the tensor spectral index n_T is found to be

$$n_T = \frac{d \ln P_T}{d \ln k} \approx 3 - \left| \frac{\bar{\epsilon} - 3}{\bar{\epsilon} - 1} \right|. \quad (170)$$

Since the fast-roll parameter is usually of $\mathcal{O}(100)$, this leads to a tensor spectral index of $n_T \approx 2$, which corresponds to a strongly blue spectrum of gravitational waves. This implies that on large scales the amplitude of gravitational waves is extremely small. For example, a gravitational wave that is roughly the size of today's horizon would have an exponentially small amplitude that is impossible to observe in the near future. At high frequencies the spectrum is cut off [38]. This can be explained by noting that after the ekpyrotic phase, as the universe becomes kinetic energy dominated, the higher-dimensional spacetime is locally equivalent to Minkowski spacetime [36]. Therefore, gravitational waves that leave the horizon during kinetic energy domination are not amplified.

5 Inflationary Cosmology versus the Cyclic Universe

In the previous sections two different cosmological models and their solutions to the standard problems of cosmology have been discussed. In section 3 the single-field model of inflation was described. Inflation can easily be incorporated into the hot big bang model, leading to the current consensus model of cosmology. In this model the universe is created at the big bang, which is followed by a brief period of rapid accelerated expansion. During this period of inflation the cosmological problems are solved and density perturbations are generated. After this phase the well-known standard big bang scenario takes over.

The second model that has been discussed is the cyclic universe. This model was investigated in section 4. Each cycle begins with a big bang at which, in this scenario, space and time remain finite. The model does not include a period of inflation, so that the radiation dominated epoch begins almost immediately after the big bang. After the standard hot big bang phase the universe enters a period of dark energy domination. This period is crucial for the success of the model. Eventually, a slowly contracting ekpyrotic phase begins during which the cosmological problems are solved and the seeds for structure formation in the next cycle are generated. The crunch ensues and the cycle begins anew.

There are a number of key differences between these two models. In the consensus model space and time have a beginning at the big bang singularity, when the universe was in a state of nearly infinite temperature and density. In contrast, the cyclic model does not postulate the existence of a beginning. It can undergo an infinite amount of cycles and is thus infinite in both space and time. The big bang in this model corresponds to a physical event, a transition from contraction to expansion at which the temperature and density remain finite. In inflationary cosmology the cosmological problems are solved by a short period of rapid expansion in the very early universe. Due to the recent discovery of dark energy [1, 2] the model also has to include a second period of accelerated expansion, whose origin is so far unexplained. The consensus model does not make a clear prediction about the future of the universe. In the cyclic model the cosmological problems are solved using a long-lasting, slowly contracting phase preceding the big bang. The model only includes one period of accelerated expansion per cycle, caused by dark energy, which is an important ingredient of the model. It does not include a period of high-

energy inflation. The cyclic model does predict the future of our universe. After an extended period of dark energy domination the universe will start contracting and is headed for a big crunch.

It has been shown that both a period of inflation in the early universe and an ekpyrotic phase preceding the big bang can solve the cosmological problems described in section 2. Most importantly, both models can predict a spectrum of nearly scale-invariant adiabatic density perturbations, as required by observations. However, both inflation and ekpyrosis face a number of challenges and are so far incomplete. In section 5.1 the main advantages and problems of the two models will be contrasted. One could limit this discussion to comparing inflation and ekpyrosis and their mechanisms of solving the cosmological problem. However, the existence of a viable model of the universe that these periods can be embedded in is crucial for their success. Therefore, in this section instead the corresponding cosmological models, the consensus model and the cyclic model, will be contrasted. In section 5.2 the predictions of the two models concerning the spectra of scalar and tensor perturbations, as well as the degree of non-gaussianity will be compared and the current observational bounds will be given. Future experiments leading to the possibility of distinguishing between the two models will be mentioned. These efforts will focus on the search for primordial gravitational waves and signatures of non-gaussianity, for both of which the two models predict very different results.

5.1 Strengths and Problems of the Models

Over the past three decades single-field inflation has become the most popular theory to describe the very early universe and is now an accepted element of the consensus model of cosmology. As demonstrated in section 3.2, inflation can explain the observed flatness and large-scale homogeneity of the universe, as well as provide an explanation for the lack of magnetic monopoles and other topological defects. Most importantly, as shown in section 3.3, during inflation a nearly scale-invariant, gaussian spectrum of curvature perturbations is generated that can provide an explanation for the origin of large-scale structure. As will be shown in section 5.2, the predicted spectrum is in excellent agreement with observations of the cosmic microwave background. Inflation has outlasted numerous competitors and predicted a nearly scale-invariant spectrum of primordial density perturbations [14, 15, 16, 17, 18] previous to the first observation of such a spectrum [4]. The production of a

spectrum of scalar perturbations similar to the inflationary spectrum now is an absolute necessity for the success of a cosmological model.

Compared to most other theories inflation has a major advantage concerning the properties of the big bang. The dynamics at the big bang singularity are unknown and until the development of a consistent theory of quantum gravity no significant progress in the understanding of the singularity can be made. In chaotic inflation no major fine-tuning of the initial conditions for the inflaton field is required [13] and inflation works practically independently of the properties of this singularity, which makes it a viable model even in the absence of a theory of quantum gravity. As long as a scalar field, initially larger than the Planckian value, with a sufficiently flat potential to allow for slow-roll can exist shortly after the big bang, inflation takes place and leads to a universe compatible with observations. Therefore, a wide range of possible pre-inflationary states exist. It should however be mentioned that inflation is geodesically incomplete towards the past [93], which implies that it does not work for completely arbitrary initial conditions.

Inflation can easily be incorporated into the standard hot big bang model. In addition to solving many of the model's problems, it also provides an explanation for the origin of radiation and elementary particles in the universe. As was briefly explained in section 3.1, in inflationary cosmology matter and radiation are created through the decay of the inflaton field during a period of reheating that takes place after the field has reached its minimum (see e.g. [46]).

Inflation and the hot big bang model offer accurate predictions and compelling explanations for the current state of the universe. The assumptions of the model are physical and agree well with observations. However, many of these assumptions are so far unproven, rendering the theory incomplete. Furthermore, besides its predictive and explanatory strength, the consensus model faces a number of conceptual problems and some of the main questions posed when inflation was first discovered are still unanswered today.

While in this review we focus on single-field chaotic inflation, numerous versions of inflation exist, some conceptually very different from the scenario described in this paper, but all agree with present observational data. Examples are for instance hybrid inflation [52, 53] which requires the presence of multiple fields, or k inflation [94] which relies on the existence of non-trivial kinetic terms in the action. Distinguishing between these models and choosing the correct one from the large number of available theories will be extremely difficult and requires much better observational techniques than

are currently available. Furthermore, instead of one period of accelerated expansion, there could be several stages of inflation, each with its own individual properties. While this is by no means a reason to abandon the theory, it would be nice to find a mechanism to narrow down the number of candidates and thus increase the predictive power of inflation.

Inflation relies on a semi-classical description of the early universe. However, for a complete theory a full quantum description is necessary. This is especially true for the investigation of quantum fluctuations during inflation. For fluctuations that have sub-Planckian wavelengths at the beginning of inflation, quantum gravity effects could be important and lead to a different spectrum than predicted by the standard inflationary model. Furthermore, attempts to embed inflation in theories of quantum gravity encountered some unexpected difficulties and even though a lot of progress has been made (for a recent review see e.g. [95]), models of inflation in string theory still face a number of serious problems.

While inflationary and big bang cosmology can accurately predict and explain many properties of our universe, the recent discovery of dark energy [1, 2] was a complete surprise. The observed cosmic acceleration was not predicted and the role dark energy plays in the model is still unclear today. To agree with observations the consensus model has to include two types of cosmic acceleration. The energy densities of these two types of inflation are different by a hundred orders of magnitude, so that so far no natural link between them could be found. The observed acceleration can be incorporated into inflationary and big bang cosmology by assuming that during reheating, in addition to matter and radiation, dark energy is produced. However, in order to achieve the correct ratios of these components, significant fine-tuning is needed. Explaining the exact value of the vacuum density is a major problem for cosmology. The vacuum density is positive, close to constant and extremely small [1, 2]. Despite many attempts, so far no convincing mechanism to explain these properties that is compatible with the consensus model has been found.

Most importantly, some of the major conceptual problems of inflationary and big bang cosmology that have been known for decades are still unsolved. The state of the universe before inflation is unknown. It is postulated that the universe starts out in an inflating state, but no explanation is offered about why it would start out in this state, how it entered the period of inflation, or what is the origin of the inflaton field. A dynamical theory proving that inflation is an attractor state in the early universe is still lacking. There is

not much hope that these issues will be resolved in the near future. While it is almost certain that inflation has to be preceded by an initial singularity, representing the origin of the universe and the beginning of time, without a theory of quantum gravity the properties and dynamics of this singularity will remain unknown. Additionally, even the nature of the inflaton field is uncertain. In this paper it has been assumed that the inflaton field is a scalar field. While most inflationary theories rely on this assumption, numerous other possibilities exist. For example, the field could be a fermionic condensate, a construct related to the curvature scalar as in Starobinsky's model [96], or have completely different properties. It can be seen that in the consensus model there are various open issues regarding the beginning and first moments of the universe. Due to the difficulties of incorporating dark energy into the model, the long-term future of the universe is just as uncertain. The resolution of these issues is crucial for developing a complete theory of the universe, however, in the last few years not much progress has been made.

Several of the above problems can be solved by anthropic arguments [97, 98]. Life can only exist in regions of the universe that fulfil the right conditions. Therefore, even if certain properties of the observable universe seem highly improbable, we are still likely to observe them, because for different properties life of this form would not exist, so that observing them is impossible. While this approach does make sense, it is uncertain if the anthropic selection mechanism is strong enough to explain all the puzzling features of our universe. Also, this approach still leaves the question of the origin of the universe unanswered. Most importantly, relying on anthropic arguments is scientifically unappealing. The argument contrasts our universe with hypothetical other universes that will never be observed and whose properties cannot be known. The argument cannot be tested experimentally and therefore will never be verified or dismissed. Clearly it would be much more favourable to solve these problems using a scientific theory that makes quantifiable predictions and can be tested.

It can be seen that inflationary and big bang cosmology still suffers from a large number of problems that have to be addressed. This does not mean that inflation is wrong. It is still the most successful model that exists. However, we should remind ourselves that so far there is no direct proof for a period of accelerated expansion in the early universe. The discussion above illustrates that the current model requires improvement and is incomplete. Therefore, despite the successes of inflation and the consensus model, alternative cosmological theories should also be explored. This is an excellent way to find

out if the predictions of inflation are truly unique. If no successful alternative is found, the confidence in inflation will be greatly increased. If a legitimate competing theory can be formulated we would enter an exciting new stage in cosmological research, trying to establish which alternative is the true model of the universe. Any alternative model must be able to solve the standard cosmological problems and to generate a spectrum of curvature perturbations that agrees with observations. One model that accomplishes this and additionally offers solutions for a variety of other problems while relying on physically plausible assumptions is the cyclic model of the universe.

As was shown in section 4.3, the cyclic model can solve the flatness, homogeneity and magnetic monopole problems of standard big bang cosmology. It can also generate a spectrum of nearly scale-invariant curvature perturbations, as was demonstrated in section 4.4. It can solve these cosmological problems without relying on a period of high-energy inflation in the early universe. Instead, it includes a period of ultra-slow contraction preceding the big bang. In the cyclic model the properties of the universe observed today are the result of such a phase of ekpyrotic contraction that occurred in the previous cycle. Ekpyrosis is a genuinely novel approach to explain the existence of a flat, homogeneous universe containing the observed large-scale structure.

One of the main strengths of the cyclic model is that it includes dark energy. In contrast to almost all other cosmological models it provides an explanation for the origin of dark energy and the corresponding cosmic acceleration. In the cyclic model this acceleration is caused by the same scalar field that drives the entire cosmic evolution. Dark energy is a vital ingredient of the model. It establishes cyclic evolution as a stable attractor solution. More importantly, an extended period of dark energy domination is required for a universe like ours to emerge after each crunch, as has been explained when discussing the phoenix universe in section 4.2. It should be noted that dark energy, a kind of low energy inflation, is not required to solve the cosmological problems. The ekpyrotic phase can achieve this on its own [70, 99]. In contrast to the consensus model, the cyclic model only requires one period of cosmic acceleration, and this acceleration has been confirmed by observations. More precisely, during the first stages of dark energy domination the cyclic model predicts an equation of state $w \approx -1$. As the scalar field rolls down the potential, w is predicted to increase. Current observational data suggests that today $w = -0.980 \pm 0.053$ [1], which agrees well with the value predicted by the cyclic model. No increase of this equation of state has been observed so far, however, according to the cyclic model such a change could most likely

only be detected on much larger time scales.

In the consensus model different issues are approached with individual theories and separate solutions. In contrast, the cyclic model provides a complete picture of cosmic evolution while relying only on branes and their motion. In the four-dimensional picture an entire cycle can be described using scalar fields evolving along a potential, so that, unlike in inflationary cosmology, the behaviour of the early universe and the late universe is determined by the same elements. The cyclic model manages to describe all phases of cosmic evolution using a simple approach that makes efficient use of the different ingredients. A detailed description of this approach was given in section 4.2. In addition to including the hot big bang phase and dark energy, the cyclic model also predicts the future of our universe. The universe will undergo an extended period of dark energy domination and then enter a slowly contracting phase which will ultimately lead to a big crunch. After this crunch the universe will start expanding again and enter a new hot big bang phase. The cycles can continue into the distant future. Equivalently, one can follow the cycling backwards in time into the infinite past, so that no explanation for the beginning of the universe or the origin of time is needed.

In the cyclic model of the universe the big crunch/big bang singularity is comparatively well understood. While in standard big bang cosmology the singularity is a mysterious moment of creation at which space and time come into existence and whose dynamics and properties are unknown, in the cyclic model the singularity corresponds to a physical event and is relatively mild. In the higher-dimensional picture the big bang occurs at the collision of two boundary branes and corresponds to a smooth transition from contraction to expansion. The collision is well-behaved and does not correspond to the beginning of time or the vanishing of the three large spatial dimensions. While there are several unresolved issues related to the big crunch/big bang transition in the cyclic model, the basics of the higher-dimensional picture are well-established [36, 65] and many efforts in string theory and M-theory are currently underway to clarify this picture (see e.g. [60, 61, 62, 63, 36, 66, 65]). A very encouraging recent development has been the investigation of a toy model of a big crunch/big bang transition in the context of AdS/CFT correspondence [100, 101]. Therefore, while the behaviour of the universe when passing through the singularity is not completely understood yet, the situation looks much more hopeful than attempts to describe the singularity in inflationary and big bang cosmology.

Compared to the consensus model of cosmology the cyclic model of the uni-

verse involves enormous time scales. These time scales can allow for new approaches to solve long outstanding cosmological problems. For example, it has been realised that the cyclic model could explain the incredibly small value of the vacuum energy density that is observed today [30, 102]. This so-called cosmological constant problem is one of the greatest challenges in physics. Previous attempts to solve this problem failed, because the required amount of tuning could not be achieved in the limited amount of time available between the big bang singularity and today. However, in the cyclic model time existed before the big bang and thus much larger time scales are involved. Therefore, this problem can be circumvented. While the details of the solution mechanism are not fully established yet, a compelling argument has been presented in [102].

The cyclic model proposes convincing solutions to the standard cosmological puzzles, as well as offering an intriguing new outlook on elements of the universe that are so far unexplained by inflationary and big bang cosmology. However, many of the model's predictions have not yet been tested. Furthermore, some of its core assumptions have been challenged and the descriptions of certain aspects of the model that are crucial to its validity are incomplete at present.

Supporters of inflationary cosmology have pointed out that the cyclic model makes some dubious assumptions. It has been questioned if particle production at the big crunch/big bang transition could really be accompanied by an increase in scalar field kinetic energy [20]. Furthermore, it has been claimed in [103] that during ekpyrosis classical field inhomogeneities could be amplified, which would lead to chaos when approaching the big crunch resulting in the breakdown of the model. Further growth of inhomogeneities is expected for models that involve more than one field [77]. Also, compared to inflationary cosmology, the generation of the correct spectrum of density perturbations in the cyclic model is more complicated. While for single-field inflation only a single phase of exponential expansion is required, the cyclic model relies on at least two fields and a two-step process, creation of entropy perturbations and conversion into curvature perturbations. Therefore, inflation might be preferable due to its simplicity and due to the fact that the success of the cyclic model relies on some unproven assumptions.

A major weak point of the cyclic model is that at present no complete theory that could underlie the braneworld scenario is known. A complete quantum theory describing this scenario is necessary for the consistency of the cyclic model. Most importantly, the cyclic potential could not yet be derived from

first principles, so that in the current model it has to be chosen by hand. The scalar potential is responsible for the entire cosmic evolution, therefore a fundamental derivation of a potential of the required shape in heterotic M-theory or a similar setting is of crucial importance. We are encouraged by the fact that in supergravity negative potentials are very natural and different possible origins of the cyclic potential have been proposed in recent years. Most importantly, the attractive force acting between the two boundary branes could be a result of virtual exchange of membranes that stretch between the branes. Some encouraging first investigations of this possibility can be found in [104, 105]. Therefore, there is hope that a potential of the required shape could soon be found. However, despite many attempts a complete derivation of the cyclic potential from a fundamental theory is still lacking.

The main challenge facing the cyclic model is the lack of nonlinear matching conditions from a contracting to an expanding universe. While classical and semi-classical analyses of the big crunch/big bang transition are well-established, a full quantum treatment is still missing. A successful transition is of crucial importance for the consistency of the cyclic model, since without a smooth transition repeating cycles are impossible. Solving the singularity problem is especially important for the validity of the theory of perturbations. It has been shown in section 4.4 that an almost scale-invariant spectrum of curvature perturbations can be generated before the big crunch. It was assumed that this spectrum is conserved when the universe passes through the bounce [27]. The success of the entire model rests on this unproven assumption. Without a full quantum treatment of the bounce this assumption cannot be proven and it is uncertain if the model can really predict the existence of a nearly scale-invariant spectrum of curvature perturbations after the big bang.

A better understanding of the cosmic singularity has to come from the higher-dimensional setting and the dynamics at the big crunch/big bang transition ultimately have to be derived from string theory. The singularity in the cyclic model has briefly been described at the beginning of section 4. The fifth dimension momentarily shrinks to zero while the three large dimensions remain finite and time continues smoothly. The brane scale factors are finite and there is no curvature singularity. However, gravitational fluctuations could be of significant size. When approaching the singularity the geometry of the universe is approximately flat [36]. Dangerous modes, if present, are diluted during the ekpyrotic phase and only start to dominate after quantum gravity becomes important [99]. Due to these properties the singularity is

one of the mildest possible and there is hope that it can soon be resolved in string theory. While much progress has been made over the past years, a formal description of the bounce within string theory is still missing and the matching rules at the brane collision could not be derived so far. Currently, experts are studying lower-dimensional toy models [100, 101, 106]. While results from these models are encouraging, the calculations are very complicated and much work is left to be done. Without a complete understanding of the dynamics at the singularity the perturbation spectrum predicted by the cyclic model remains questionable. Without a consistent quantum theory even the matching of basic properties of the universe across the crunch is uncertain. This could affect the predictions of flatness and homogeneity. Therefore, a quantum theory describing the dynamics at the bounce is urgently needed for a consistent formulation of the cyclic model. Without such a theory the model's predictions are not reliable.

It can be seen that, while the cyclic model is a promising candidate for an alternative model to inflationary cosmology, much work remains to be done. Given that this model has only been proposed a few years ago and that it is competing with a model that has been carefully studied for almost thirty years, this should not come as a surprise.

It can be concluded that both the consensus model and the cyclic model offer physically plausible and convincing explanations for the state of our universe. However, both models still contain a large number of open issues and need to be improved. Ultimately, the correct model will be determined from observations. Therefore, in the following section the experimentally testable predictions of the models are compared, recent experimental data is given and potentially significant future developments are discussed.

5.2 Experimentally Testable Predictions

In section 3.3 and section 4.4 the predictions of the inflationary and cyclic models for the perturbation spectra have been given, respectively. In the following these predictions will be compared with observational data. First, the results for scalar perturbations will be discussed, then we will comment on the degree of non-gaussianity predicted by each of the models and finally the generated spectra of gravitational waves will be compared.

Scalar perturbations

The scale-dependence of the spectrum of scalar perturbations can be quantified by the scalar spectral index n_S . For single-field inflation this spectrum has been analysed to linear order in the perturbations and the spectral index n_S^{inf} was found in (76). It is given by

$$n_S^{inf} \approx 1 - 4\epsilon - 2\delta. \quad (171)$$

This expression is to lowest order in the slow-roll parameters ϵ and δ , which were defined in (26). Since during inflation these parameters are much smaller than unity, the spectrum of scalar perturbations is close to scale invariant. ϵ is always positive, while δ can have either sign. Therefore, in theory n_S^{inf} can be slightly larger or slightly smaller than unity. In practice most inflationary models predict a red-tilted spectrum. This can be seen explicitly by considering the example of power law inflation. In this scenario the scale factor grows as some power of time $a(t) \propto t^q$, where q is a positive constant. This implies that the Hubble parameter is given by $H(t) = q/t$. Using the equations of motion during inflation that are given in (22) and (23) explicit expressions for the slow-roll parameters in power law inflation can be found. They are given by

$$\epsilon = \frac{1}{q}, \quad \delta = -\frac{1}{q}. \quad (172)$$

After inserting this into (171) the spectral index predicted by power law inflation is found to be

$$n_S^{inf} = 1 - \frac{2}{q}. \quad (173)$$

Since $q > 0$, the spectral index $n_S^{inf} < 1$, which corresponds to a red-tilted spectrum. Also, since during inflation the scale factor is rapidly increasing, q must be quite large, so that the deviation from scale invariance is small. This is of course just a basic example. However, the simplest versions of chaotic inflation make similar predictions for the properties of the scalar perturbation spectrum. While the exact value of n_S^{inf} depends on the shape of the potential in the investigated model, in general it can be said that single-field inflation predicts a nearly flat, slightly red-tilted spectrum of adiabatic perturbations. The scalar spectral index in these models falls roughly within the range $0.92 \leq n_S^{inf} \leq 0.97$ [107]. It should be noted that these predictions can be violated in more complicated versions of inflation that include additional scalar fields or complicated potentials.

The scale-dependence of the spectrum of entropy perturbations generated during the ekpyrotic phase, resulting from the analysis of perturbations to linear order, has been found in (152). It was shown in the large-scale approximation that these entropy perturbations can be converted into curvature perturbations with exactly the same spectrum. Therefore, the curvature perturbations inherit the spectral index from the entropy perturbation spectrum. The scalar spectral index predicted by the cyclic model, n_S^{ekp} , is thus given by

$$n_S^{ekp} \approx 1 + \frac{2}{\bar{\epsilon}} - \frac{\bar{\epsilon}_{,M}}{\bar{\epsilon}^2}, \quad (174)$$

where $\bar{\epsilon}$ is the fast-roll parameter defined in (106) and M is related to the logarithm of the scale factor as $M = \ln(a(t)/a(t_{end}^{ek}))$. The second term on the right-hand side is a gravitational contribution. Since it is positive it tends to make the spectrum blue. The third term on the right-hand side is a non-gravitational contribution which tends to make the spectrum red. For an exponential potential one can use the scaling solution in (104). The fast-roll parameter is then given by $\bar{\epsilon} = 1/p$, and in this approximation $p > 0$ is a constant. The non-gravitational contribution to the spectral index vanishes and (174) becomes

$$n_S^{ekp} = 1 + 2p. \quad (175)$$

This clearly corresponds to a blue spectrum. During ekpyrosis the scale factor is slowly varying, so that $p \ll 1$. Therefore, the spectrum is close to scale invariant. For more general potentials the non-gravitational term can become important, so that some cyclic models predict a red-tilted spectrum. In fact, $\bar{\epsilon}_{,M} = 0$ is an unrealistic statement, since the steepness of the potential has to decrease for the ekpyrotic phase to end and kinetic energy domination to take over. While the precise value of the spectral index depends on the shape of the potential, the predictions of the simplest cyclic models roughly fall within the range $0.97 < n_S^{ekp} < 1.02$ [28]. Therefore, this model can lead to both slightly blue and slightly red spectra of scalar perturbations. It should be noted that methods of generating curvature perturbations other than the entropic mechanism are still considered, some of which can lead to a range of n_S^{ekp} that is shifted to slightly lower values (see e.g. [108]).

Comparing this with the predictions for the spectral index from single-field inflation it can be seen that both models lead to a nearly flat spectrum of curvature perturbations. The predicted range of values for the scalar spectral index in the cyclic model is shifted slightly to the blue compared to the values permitted by inflation. Therefore, a highly precise measurement of the scalar spectral index could provide an indication as to which of the two models more accurately predicts the properties of our universe.

The bound on the scalar spectral index of the power spectrum of primordial curvature perturbations from seven-year WMAP data combined with BAO and H_0 measurements is $n_S = 0.963 \pm 0.012$ [3]. It can be seen that, within the error range, both inflationary and cyclic models can satisfy this constraint. A blue spectrum is experimentally ruled out, such that a purely exponential ekpyrotic potential can be excluded. However, as stated above, such a potential was already disfavoured due to theoretical considerations. The observed spectral index is slightly more compatible with the range predicted by single-field inflation. Overall however, based on this observed value none of the two models has a clear advantage. It could even be argued that both of the models gain credibility for being able to satisfy this relatively stringent constraint. While the error bars might shrink in the future, to be able to determine which of the two models is more realistic other experimentally testable predictions should also be compared.

Non-gaussianity

The non-gaussian contribution to the spectrum of scalar perturbations in simple, single-field inflationary models is very small. As estimated in section 3.3 these models predict an approximate value of $|f_{NL}^{inf}| \leq 1$. This level of non-gaussianity is extremely small, so that it cannot be detected in near-future experiments. It should be noted that inflationary models that include multiple fields or complex kinetic terms are able to generate a significantly larger amount of non-gaussianity [57, 58, 59].

A significant level of non-gaussianity is an important prediction of the cyclic model of the universe. In this model the non-gaussianity parameter f_{NL}^{ekp} is usually of order a few tens and can have either sign. It is predicted to roughly fall in the range $-60 \leq f_{NL}^{ekp} \leq +80$ [109], the exact value depends on the details of the conversion from entropy to curvature perturbations. Therefore, in the cyclic model obtaining a value of $|f_{NL}^{ekp}| \approx 1$ is very unnatural. Typical values of f_{NL}^{ekp} are more than an order of magnitude larger than the values obtained in single-field inflation. It should also be noted that there is a correlation between f_{NL}^{ekp} and the spectral index. A relatively red spectrum of curvature perturbations implies a large amount of non-gaussianity. Given the discussion of the scalar spectral index in the previous section it can be expected that a significant amount of non-gaussianity is generated in the cyclic model.

It can be seen that very different levels of non-gaussianity are predicted by

single-field inflation and the cyclic model. This makes the non-gaussian contribution to the spectrum of scalar perturbations one of the most important probes of the very early universe. A detection of primordial non-gaussianity with $f_{NL} \gg 1$ would immediately rule out the single-field inflationary scenario. Even though more complicated models of inflation could account for such a discovery, this would require fine-tuning of the parameters. In contrast, the presence of a significant amount of non-gaussianity is completely natural in the cyclic model. The constraint on local non-gaussianity by seven-year WMAP data combined with SDSS data is $-5 < f_{NL}^{local} < 59$ [19]. This constraint allows for both an almost perfectly gaussian spectrum of curvature perturbations as predicted by single-field inflation, as well as the levels of non-gaussianity that are generated in the cyclic model. It should be noted that the largest possible amounts of non-gaussianity in the cyclic model are observationally excluded, which by some is seen as supporting single-field inflationary models. On the other hand, recently the detection of a primordial signal of local non-gaussianity was claimed [110], which can be explained by the cyclic model but by far exceeds the value predicted by single-field inflation. While there is some doubt about the validity of this discovery, it is an encouraging development for supporters of the cyclic universe.

In conclusion, current observational data of primordial non-gaussianity can be explained by both cyclic and single-field inflationary models. Uncertainties in the measurements will improve dramatically as soon as data from the Planck satellite becomes available. In this experiment values as small as $|f_{NL}| \geq 5$ could be detected. If a non-gaussian signature is found by the Planck satellite mission this will strongly support the cyclic model. If no such signature is detected, inflationary cosmology is favoured by the data. This is encouraging. In a couple of years we should have a strong indication which of the two theories is correct. To establish the favoured theory as the valid cosmological model the experimental search for gravitational waves will be of crucial importance.

Tensor perturbations

The spectral index characterising the spectrum of tensor perturbations in single-field inflation has been found in (96) and, to lowest order in the slow-roll parameters, is given by

$$n_T^{inf} \approx -2\epsilon. \quad (176)$$

Here, ϵ is the slow-roll parameter defined in (26). A scale-invariant spectrum would correspond to $n_T^{inf} = 0$. Since ϵ is much smaller than unity during inflation, the predicted spectrum of tensor perturbations is nearly scale-invariant. Because $\epsilon > 0$, the tensor spectral index $n_T^{inf} < 0$, so that the deviation from a flat spectrum is due to a slight tilt to the red. Therefore, single-field inflationary models predict a slightly red, nearly scale-invariant spectrum of gravitational waves. The exact value of n_T^{inf} depends on the shape of the potential.

An important observational quantity is the tensor to scalar ratio r which was defined in (97) and is related to n_T^{inf} as shown in (98). Therefore,

$$r = 16\epsilon = -8n_T^{inf}. \quad (177)$$

This is known as the consistency relation and holds for single-field inflation. Since $\epsilon \ll 1$ it can be seen that the amplitude of gravitational waves is much smaller than the amplitude of scalar perturbations. This relation does not apply in models of inflation that involve more than one field. Single-field inflationary scenarios usually predict the scalar to tensor ratio to be within the range $0 \leq r \leq 0.3$. While this is not very restrictive, it has been argued that, for inflationary models that satisfy $n_S^{inf} \geq 0.95$ and are thus consistent with observations, a value of $r \geq 10^{-2}$ can be expected [111]. While this is a well-justified lower limit, there exist a number exceptions to this statement. In a few models of inflation the amplitude of the generated gravitational waves is so small that it is undetectable in the near future. This is especially true for string theory inflation models [112].

The tensor spectral index predicted by the cyclic model of the universe was calculated in (170) and is given by

$$n_T^{ekp} \approx 3 - \left| \frac{\bar{\epsilon} - 3}{\bar{\epsilon} - 1} \right|, \quad (178)$$

where $\bar{\epsilon}$ is the fast-roll parameter defined in (106). Since ϵ is of $\mathcal{O}(100)$, this gives a tensor spectral index of approximately $n_T^{ekp} \approx 2$, which corresponds to a strongly blue spectrum of gravitational waves. The amplitude of these gravity waves is extremely small on large scales. In fact, on the largest observable scales the dominant contribution to the amplitude is expected to result from the backreaction of the scalar fluctuations onto the geometry [113]. Therefore, according to this model primordial gravitational waves will most likely never be detected.

Compared to inflationary models the amplitude of gravitational waves on large scales in the cyclic model is strongly suppressed. While inflation pre-

dicts a nearly scale-invariant, slightly red spectrum of tensor perturbations, the spectrum in cyclic models is very blue with an amplitude that is orders of magnitude too low to be detected by current and near-future experiments. Therefore, gravity waves are probably the most important observational test to distinguish between single-field inflation and the cyclic model. A detection of an imprint of tensor perturbations in the polarization of the cosmic microwave background is consistent with inflationary models, but cannot be explained by cyclic models. Such a detection would unambiguously rule out the ekpyrotic and cyclic scenarios.

Unfortunately, so far not much data is available. Gravitational waves have not yet been detected and therefore no observational constraints on the tensor spectral index n_T exist. Seven-year WMAP results combined with BAO and H_0 measurements suggest that $r < 0.24$ at the 95% confidence level [3]. This is easily compatible with both inflationary cosmology and the cyclic model. However, the situation might improve in the near future. For high enough amplitudes the Planck satellite mission might detect indirect proof for primordial gravitational waves imprinted on the CMB. If gravitational waves are detected, their amplitude can be measured and the spectral index can be found, then the consistency relation (177) could be tested. The confirmation of this relation would be an incredible success for single-field inflation and once and for all establish it as the model describing the very early universe. It should be noted that, while the absence of gravitational waves would focus much attention on the cyclic model, it would not altogether rule out the concept of inflation, since several inflationary scenarios are able to produce gravity waves with an unobservably small amplitude.

There are several other ways to distinguish between single-field inflationary cosmology and the cyclic model that have not been discussed here. The running of the scalar spectral index has been ignored, because so far there is no observational evidence that this quantity is significant. Non-gaussianity in inflationary and cyclic models could be further contrasted by investigating the third-order nonlinearity parameter g_{NL} . However, no strong observational constraints on this value exist so far. It has also recently been pointed out that some cyclic models predict a spatial variation of dark energy in the universe [31]. This could be further investigated.

6 Conclusions

In this paper two competing cosmological models have been presented. While the models are conceptually very different, they both agree well with observations. The consensus model combines the hot big bang model with a period of inflation in the early universe. The cyclic model predicts a cyclic evolution with each cycle including a slowly contracting ekpyrotic phase. Both inflation and the ekpyrotic phase can solve the standard cosmological problems and lead to the generation of a nearly scale-invariant spectrum of curvature perturbations. While both models offer accurate predictions and physically plausible explanations for the observed state of the universe, each model faces some conceptual problems.

The main shortcoming of the cyclic model is the lack of a complete quantum description. A derivation of the cyclic potential from a fundamental theory has so far not been possible and without a quantum theory the dynamics of the bounce cannot be fully understood. Observational predictions of the cyclic model heavily rely on the assumption that perturbations are conserved when passing through the singularity. Without a proof of this behaviour the predictions of the model are not reliable. The dynamics of the singularity are also unknown in the consensus model. However, inflation can work almost independently of these dynamics and the predictions of the model do not rely on them. Therefore, even though finding an embedding in a theory of quantum gravity is important for the consistency of both cosmological models, only the cyclic model loses credibility due to the lack of it. While efforts are currently underway to develop a complete description of the bounce in string theory and much progress has already been made, until such a description is found the model is incomplete.

Inflationary cosmology suffers from its own conceptual problems. The origin and nature of the inflaton field are unknown and how the universe entered inflation is unexplained. The future of the universe is equally uncertain. In contrast, the cyclic model provides a complete picture of cosmic evolution. Dark energy is an important ingredient of the model, while its role in the consensus model is unclear. However, the success of the cyclic model depends on the validity of unproven assumptions. In contrast, once the universe has entered inflation the dynamics are well-understood, so that reliable predictions can be made.

While both models are very appealing, inflationary cosmology seems to be better understood. This is not surprising. Inflation has been around for

decades, while the cyclic model is a relatively new theory which is still in full development. Much effort is made to improve it and there is hope that its main problems can soon be solved. Ultimately, the correct model will be determined from observations. While inflationary cosmology and the cyclic model both predict a nearly scale-invariant spectrum of curvature perturbations, the models differ in their predictions of non-gaussianity and gravitational waves. Single-field inflation leads to undetectably small non-gaussian corrections and a nearly scale-invariant, slightly red-tilted spectrum of gravitational waves. In contrast, the cyclic model predicts a strong non-gaussian signature which could soon be detected, while the gravitational wave spectrum is very blue, with unobservably small amplitudes on large scales.

Both the cyclic model and inflationary cosmology are compatible with current observations. This could change when data from the Planck satellite mission becomes available. The Planck satellite can detect small levels of non-gaussianity and could observe an imprint of primordial gravitational waves on the cosmic microwave background. The discovery of a strong non-gaussian signal would rule out single-field inflation. The lack of such a signal would disfavour the cyclic model and a detection of gravitational waves would unambiguously rule it out. Both the absence of gravitational waves and a non-gaussian signal would support the cyclic model, but could also be explained by more complicated models of inflation. However, this would require fine-tuning, while in the cyclic model these results occur naturally.

This is a very exciting time for cosmologists. Within a couple of years observational data will give a strong indication of whether inflationary cosmology or the cyclic model more accurately predicts the state of our universe.

References

- [1] S. Perlmutter et al. Measurements of Omega and Lambda from 42 High-Redshift Supernovae. *Astrophys. J.*, 517:565–586, 1999.
- [2] A. G. Riess et al. Observational Evidence from Supernovae for an Accelerating Universe and a Cosmological Constant. *Astron. J.*, 116:1009–1038, 1998.
- [3] N. Jarosik et al. Seven-Year Wilkinson Microwave Anisotropy Probe (WMAP) Observations: Sky Maps, Systematic Errors, and Basic Results. 2010.
- [4] G. F. Smoot et al. Structure in the COBE differential microwave radiometer first year maps. *Astrophys. J.*, 396:L1–L5, 1992.
- [5] C. L. Bennett et al. 4-Year COBE DMR Cosmic Microwave Background Observations: Maps and Basic Results. *Astrophys. J.*, 464:L1–L4, 1996.
- [6] A. H. Guth. Inflationary universe: A possible solution to the horizon and flatness problems. *Phys. Rev. D*, 23(2):347–356, Jan 1981.
- [7] S. W. Hawking, I. G. Moss, and J. M. Stewart. Bubble collisions in the very early universe. *Phys. Rev. D*, 26(10):2681–2693, Nov 1982.
- [8] A. H. Guth and E. J. Weinberg. Could the universe have recovered from a slow first-order phase transition? *Nuclear Physics B*, 212(2):321 – 364, 1983.
- [9] A. D. Linde. A new inflationary universe scenario: A possible solution of the horizon, flatness, homogeneity, isotropy and primordial monopole problems. *Physics Letters B*, 108(6):389 – 393, 1982.
- [10] A. D. Linde. Coleman-weinberg theory and the new inflationary universe scenario. *Physics Letters B*, 114(6):431 – 435, 1982.
- [11] A. D. Linde. Scalar field fluctuations in the expanding universe and the new inflationary universe scenario. *Physics Letters B*, 116(5):335 – 339, 1982.
- [12] A. Albrecht and P. J. Steinhardt. Cosmology for grand unified theories with radiatively induced symmetry breaking. *Phys. Rev. Lett.*, 48(17):1220–1223, Apr 1982.

- [13] A. D. Linde. Chaotic inflation. *Physics Letters B*, 129(3-4):177 – 181, 1983.
- [14] V. F. Mukhanov and G. V. Chibisov. Quantum fluctuations and a non-singular universe. *ZhETF Pis ma Redaktsiu*, 33:549–553, May 1981.
- [15] S. W. Hawking. The development of irregularities in a single bubble inflationary universe. *Physics Letters B*, 115(4):295 – 297, 1982.
- [16] A. A. Starobinsky. Dynamics of phase transition in the new inflationary universe scenario and generation of perturbations. *Physics Letters B*, 117(3-4):175 – 178, 1982.
- [17] A. H. Guth and S.-Y. Pi. Fluctuations in the new inflationary universe. *Phys. Rev. Lett.*, 49(15):1110–1113, Oct 1982.
- [18] J. M. Bardeen, P. J. Steinhardt, and M. S. Turner. Spontaneous creation of almost scale-free density perturbations in an inflationary universe. *Phys. Rev. D*, 28(4):679–693, Aug 1983.
- [19] E. Komatsu et al. Seven-Year Wilkinson Microwave Anisotropy Probe (WMAP) Observations: Cosmological Interpretation. 2010.
- [20] A. D. Linde. Inflationary theory versus ekpyrotic / cyclic scenario. 2002.
- [21] J. Khoury, B. A. Ovrut, P. J. Steinhardt, and Neil Turok. The ekpyrotic universe: Colliding branes and the origin of the hot big bang. *Phys. Rev.*, D64:123522, 2001.
- [22] A. Lukas, B. A. Ovrut, K. S. Stelle, and D. Waldram. Heterotic M-theory in five dimensions. *Nucl. Phys.*, B552:246–290, 1999.
- [23] A. Lukas, B. A. Ovrut, K. S. Stelle, and D. Waldram. The universe as a domain wall. *Phys. Rev.*, D59:086001, 1999.
- [24] A. Lukas, B. A. Ovrut, and D. Waldram. On the four-dimensional effective action of strongly coupled heterotic string theory. *Nucl. Phys.*, B532:43–82, 1998.
- [25] P. Horava and E. Witten. Heterotic and type I string dynamics from eleven dimensions. *Nucl. Phys.*, B460:506–524, 1996.
- [26] Petr Horava and Edward Witten. Eleven-Dimensional Supergravity on a Manifold with Boundary. *Nucl. Phys.*, B475:94–114, 1996.

- [27] P. Creminelli, A. Nicolis, and M. Zaldarriaga. Perturbations in bouncing cosmologies: Dynamical attractor vs scale invariance. *Phys. Rev.*, D71:063505, 2005.
- [28] J.-L. Lehners, P. McFadden, N. Turok, and P. J. Steinhardt. Generating ekpyrotic curvature perturbations before the big bang. *Phys. Rev.*, D76:103501, 2007.
- [29] P. J. Steinhardt and N. Turok. A cyclic model of the universe. 2001.
- [30] P. J. Steinhardt and N. Turok. Cosmic evolution in a cyclic universe. *Phys. Rev.*, D65:126003, 2002.
- [31] J.-L. Lehners and P. J. Steinhardt. Dark Energy and the Return of the Phoenix Universe. *Phys. Rev.*, D79:063503, 2009.
- [32] J.-L. Lehners, P. J. Steinhardt, and N. Turok. The Return of the Phoenix Universe. *Int. J. Mod. Phys.*, D18:2231–2235, 2009.
- [33] E. I. Buchbinder, J. Khoury, and B. A. Ovrut. New Ekpyrotic Cosmology. *Phys. Rev.*, D76:123503, 2007.
- [34] R. Kallosh, J. U. Kang, A. D. Linde, and V. Mukhanov. The New Ekpyrotic Ghost. *JCAP*, 0804:018, 2008.
- [35] B.K. Xue and P. J. Steinhardt. Unstable growth of curvature perturbation in non-singular bouncing cosmologies. 2010.
- [36] J. Khoury, B. A. Ovrut, N. Seiberg, P. J. Steinhardt, and N. Turok. From big crunch to big bang. *Phys. Rev.*, D65:086007, 2002.
- [37] J.-L. Lehners and S. Renaux-Petel. Multifield Cosmological Perturbations at Third Order and the Ekpyrotic Trispectrum. *Phys. Rev.*, D80:063503, 2009.
- [38] L. A. Boyle, P. J. Steinhardt, and N. Turok. The cosmic gravitational wave background in a cyclic universe. *Phys. Rev.*, D69:127302, 2004.
- [39] D. Baumann. TASI Lectures on Inflation. 2009.
- [40] A. D. Linde. Inflationary Cosmology. *Lect. Notes Phys.*, 738:1–54, 2008.
- [41] J.-L. Lehners. Ekpyrotic and Cyclic Cosmology. *Phys. Rept.*, 465:223–263, 2008.

- [42] C. L. Bennett et al. First Year Wilkinson Microwave Anisotropy Probe (WMAP) Observations: Preliminary Maps and Basic Results. *Astrophys. J. Suppl.*, 148:1, 2003.
- [43] Ya. B. Zeldovich and M. Yu. Khlopov. On the concentration of relic magnetic monopoles in the universe. *Physics Letters B*, 79(3):239 – 241, 1978.
- [44] J. Preskill. Magnetic monopoles. *Annual Review of Nuclear and Particle Science*, 34(1):461–530, 1984.
- [45] K. Nakamura et al. Magnetic Monopole Searches. *J. Phys. G* 37, 075021, 2010.
- [46] B. A. Bassett, S. Tsujikawa, and D. Wands. Inflation dynamics and reheating. *Rev. Mod. Phys.*, 78:537–589, 2006.
- [47] A. R. Liddle and D. H. Lyth. *Cosmological inflation and large-scale structure*. Cambridge University Press, 2000.
- [48] A. Riotto. Inflation and the theory of cosmological perturbations. 2002.
- [49] V. F. Mukhanov, H. A. Feldman, and R. H. Brandenberger. Theory of cosmological perturbations. Part 1. Classical perturbations. Part 2. Quantum theory of perturbations. Part 3. Extensions. *Phys. Rept.*, 215:203–333, 1992.
- [50] H. Kodama and M. Sasaki. Cosmological perturbation theory. *Progress of Theoretical Physics Supplement*, 78:1–166, 1984.
- [51] J. M. Bardeen. Gauge-invariant cosmological perturbations. *Phys. Rev. D*, 22(8):1882–1905, Oct 1980.
- [52] A. D. Linde. Hybrid inflation. *Phys. Rev.*, D49:748–754, 1994.
- [53] E. J. Copeland, A. R. Liddle, D. H. Lyth, E. D. Stewart, and D. Wands. False vacuum inflation with Einstein gravity. *Phys. Rev.*, D49:6410–6433, 1994.
- [54] J. M. Maldacena. Non-Gaussian features of primordial fluctuations in single field inflationary models. *JHEP*, 05:013, 2003.
- [55] V. Acquaviva, N. Bartolo, S. Matarrese, and A. Riotto. Second-order cosmological perturbations from inflation. *Nucl. Phys.*, B667:119–148, 2003.

- [56] D. Seery and J. E. Lidsey. Non-gaussianity from the inflationary trispectrum. *JCAP*, 0701:008, 2007.
- [57] D. H. Lyth and Y. Rodriguez. The inflationary prediction for primordial non-gaussianity. *Phys. Rev. Lett.*, 95:121302, 2005.
- [58] D. H. Lyth and Y. Rodriguez. Non-gaussianity from the second-order cosmological perturbation. *Phys. Rev.*, D71:123508, 2005.
- [59] G. Panotopoulos. Detectable primordial non-gaussianities and gravitational waves in k-inflation. *Phys. Rev.*, D76:127302, 2007.
- [60] N. Turok, M. Perry, and P. J. Steinhardt. M theory model of a big crunch / big bang transition. *Phys. Rev.*, D70:106004, 2004.
- [61] B. Craps. Big bang models in string theory. *Class. Quant. Grav.*, 23:S849–S881, 2006.
- [62] G. Niz and N. Turok. Classical propagation of strings across a big crunch / big bang singularity. *Phys. Rev.*, D75:026001, 2007.
- [63] B. Craps and B. A. Ovrut. Global fluctuation spectra in big crunch / big bang string vacua. *Phys. Rev.*, D69:066001, 2004.
- [64] Lorenzo Cornalba and Miguel S. Costa. Time-dependent orbifolds and string cosmology. *Fortsch. Phys.*, 52:145–199, 2004.
- [65] J.-L. Lehners, P. McFadden, and N. Turok. Colliding Branes in Heterotic M-theory. *Phys. Rev.*, D75:103510, 2007.
- [66] J.-L. Lehners, P. McFadden, and N. Turok. Effective Actions for Heterotic M-Theory. *Phys. Rev.*, D76:023501, 2007.
- [67] J. Khoury, B. A. Ovrut, P. J. Steinhardt, and N. Turok. Density perturbations in the ekpyrotic scenario. *Phys. Rev.*, D66:046005, 2002.
- [68] S. Gratton, J. Khoury, P. J. Steinhardt, and N. Turok. Conditions for generating scale-invariant density perturbations. *Phys. Rev.*, D69:103505, 2004.
- [69] J. Khoury, P. J. Steinhardt, and N. Turok. Designing Cyclic Universe Models. *Phys. Rev. Lett.*, 92:031302, 2004.
- [70] J. K. Erickson, S. Gratton, P. J. Steinhardt, and N. Turok. Cosmic Perturbations Through the Cyclic Ages. *Phys. Rev.*, D75:123507, 2007.

- [71] D. H. Lyth. The primordial curvature perturbation in the ekpyrotic universe. *Phys. Lett.*, B524:1–4, 2002.
- [72] R. Brandenberger and F. Finelli. On the spectrum of fluctuations in an effective field theory of the ekpyrotic universe. *JHEP*, 11:056, 2001.
- [73] P. L. McFadden, N. Turok, and P. J. Steinhardt. Solution of a braneworld big crunch / big bang cosmology. *Phys. Rev.*, D76:104038, 2007.
- [74] A. J. Tolley, N. Turok, and P. J. Steinhardt. Cosmological perturbations in a big crunch / big bang space-time. *Phys. Rev.*, D69:106005, 2004.
- [75] F. Finelli. Assisted contraction. *Phys. Lett.*, B545:1–7, 2002.
- [76] A. Notari and A. Riotto. Isocurvature perturbations in the ekpyrotic universe. *Nucl. Phys.*, B644:371–382, 2002.
- [77] K. Koyama and D. Wands. Ekpyrotic collapse with multiple fields. *JCAP*, 0704:008, 2007.
- [78] K. Koyama, S. Mizuno, and D. Wands. Curvature perturbations from ekpyrotic collapse with multiple fields. *Class. Quant. Grav.*, 24:3919–3932, 2007.
- [79] C. Gordon, D. Wands, B. A. Bassett, and R. Maartens. Adiabatic and entropy perturbations from inflation. *Phys. Rev.*, D63:023506, 2001.
- [80] A. J. Tolley and D. H. Wesley. Scale-invariance in expanding and contracting universes from two-field models. *JCAP*, 0705:006, 2007.
- [81] T. Battefeld. Modulated Perturbations from Instant Preheating after new Ekpyrosis. *Phys. Rev.*, D77:063503, 2008.
- [82] J.-L. Lehners and P. J. Steinhardt. Intuitive understanding of non-gaussianity in ekpyrotic and cyclic models. *Phys. Rev.*, D78:023506, 2008.
- [83] J.-L. Lehners and N. Turok. Bouncing Negative-Tension Branes. *Phys. Rev.*, D77:023516, 2008.
- [84] T. Banks and M. Dine. Couplings and Scales in Strongly Coupled Heterotic String Theory. *Nucl. Phys.*, B479:173–196, 1996.

- [85] J. Martin and P. Peter. On the properties of the transition matrix in bouncing cosmologies. *Phys. Rev.*, D69:107301, 2004.
- [86] R. Durrer and F. Vernizzi. Adiabatic perturbations in pre big bang models: Matching conditions and scale invariance. *Phys. Rev.*, D66:083503, 2002.
- [87] J. Martin, P. Peter, N. Pinto Neto, and D. J. Schwarz. Passing through the bounce in the ekpyrotic models. *Phys. Rev.*, D65:123513, 2002.
- [88] A. J. Tolley and N. Turok. Quantum fields in a big crunch / big bang spacetime. *Phys. Rev.*, D66:106005, 2002.
- [89] J. Hwang and H. Noh. Non-singular big-bounces and evolution of linear fluctuations. *Phys. Rev.*, D65:124010, 2002.
- [90] T. J. Battefeld, S. P. Patil, and R. Brandenberger. Perturbations in a bouncing brane model. *Phys. Rev.*, D70:066006, 2004.
- [91] J.-L. Lehners. Ekpyrotic Non-Gaussianity – A Review. *Adv. Astron.*, 2010:903907, 2010.
- [92] D. Babich, P. Creminelli, and M. Zaldarriaga. The shape of non-Gaussianities. *JCAP*, 0408:009, 2004.
- [93] A. Borde, A. H. Guth, and A. Vilenkin. Inflationary space-times are incomplete in past directions. *Phys. Rev. Lett.*, 90:151301, 2003.
- [94] C. Armendariz-Picon, T. Damour, and V. F. Mukhanov. k-Inflation. *Phys. Lett.*, B458:209–218, 1999.
- [95] D. Baumann and L. McAllister. Advances in Inflation in String Theory. *Ann. Rev. Nucl. Part. Sci.*, 59:67–94, 2009.
- [96] A. A. Starobinsky. A new type of isotropic cosmological models without singularity. *Physics Letters B*, 91(1):99 – 102, 1980.
- [97] B. Carter. Large number coincidences and the anthropic principle in cosmology. In *IAU Symposium 63: Confrontation of cosmological theories with observational data*, pages 291–298. Dordrecht: Reidel, 1974.
- [98] S. Weinberg. Anthropic bound on the cosmological constant. *Phys. Rev. Lett.*, 59(22):2607–2610, Nov 1987.

- [99] J. K. Erickson, D. H. Wesley, P. J. Steinhardt, and N. Turok. Kasner and mixmaster behavior in universes with equation of state $w = 1$. *Phys. Rev.*, D69:063514, 2004.
- [100] B. Craps, T. Hertog, and N. Turok. Quantum Resolution of Cosmological Singularities using AdS/CFT. 2007.
- [101] N. Turok, B. Craps, and T. Hertog. From Big Crunch to Big Bang with AdS/CFT. 2007.
- [102] P. J. Steinhardt and N. Turok. Why the cosmological constant is small and positive. *Science*, 312:1180–1182, 2006.
- [103] R. Kallosh, L. Kofman, and A. D. Linde. Pyrotechnic universe. *Phys. Rev.*, D64:123523, 2001.
- [104] G. W. Moore, G. Peradze, and N. Saulina. Instabilities in heterotic M-theory induced by open membrane instantons. *Nucl. Phys.*, B607:117–154, 2001.
- [105] E. Lima, B. A. Ovrut, J. Park, and R. Reinbacher. Non-perturbative superpotential from membrane instantons in heterotic M-theory. *Nucl. Phys.*, B614:117–170, 2001.
- [106] H. Liu, G. W. Moore, and N. Seiberg. Strings in a time-dependent orbifold. *JHEP*, 06:045, 2002.
- [107] V. Mukhanov. *Physical foundations of cosmology*, page 347. Cambridge University Press, 2005.
- [108] J. Khoury, P. J. Steinhardt, and N. Turok. Great expectations: Inflation versus cyclic predictions for spectral tilt. *Phys. Rev. Lett.*, 91:161301, 2003.
- [109] J.-L. Lehners and P. J. Steinhardt. Non-Gaussian Density Fluctuations from Entropically Generated Curvature Perturbations in Ekpyrotic Models. *Phys. Rev.*, D77:063533, 2008.
- [110] A. P. S. Yadav and B. D. Wandelt. Evidence of Primordial Non-Gaussianity (f_{NL}) in the Wilkinson Microwave Anisotropy Probe 3-Year Data at 2.8σ . *Phys. Rev. Lett.*, 100:181301, 2008.
- [111] L. A. Boyle, P. J. Steinhardt, and N. Turok. Inflationary predictions reconsidered. *Phys. Rev. Lett.*, 96:111301, 2006.

- [112] R. Kallosh and A. D. Linde. Testing String Theory with CMB. *JCAP*, 0704:017, 2007.
- [113] D. Baumann, P. J. Steinhardt, K. Takahashi, and K. Ichiki. Gravitational Wave Spectrum Induced by Primordial Scalar Perturbations. *Phys. Rev.*, D76:084019, 2007.